

## **Chapter 3: Instrumental Climate**

Ingeborg Auer, Reinhard Böhm and Wolfgang Schöner  
Central Institute for Meteorology and Geodynamics (ZAMG)  
Vienna, Austria

### **Contents:**

- 3.0. Introduction
- 3.1. RSC: Recent site climatology
  - 3.1.1. Data
  - 3.1.2. Temperature
  - 3.1.3. Precipitation
  - 3.1.4. Temperature at Precipitation days
  - 3.1.5. Wind
  - 3.1.6. Air pressure
  - 3.1.7. Humidity
  - 3.1.8. Snow depth
  - 3.1.9. Conclusions RSC
- 3.2. HSC: Historic site climatology
  - 3.2.1. Homogenising
  - 3.2.2. Gridding
  - 3.2.3. The gridded datasets
  - 3.2.4. First analyses of the new datasets
    - 3.2.4.1. Instrumental temperature variability in the greater Alpine region (GAR) since 1760
    - 3.2.4.2. Instrumental precipitation variability in the greater Alpine region (GAR) since 1803
    - 3.2.4.3. Spatial representativity of Alpine temperature series for Europe
    - 3.2.4.4. Series of temperature on precipitation days
    - 3.2.4.5. Series of vertical temperature lapse rates
    - 3.2.4.6. Change of the zero degree altitude
  - 3.2.5. Conclusions HSC
- 4. References

### 3.0. Introduction

The instrumental climate support study of ALPCLIM intended to

- provide the other groups on demand with instrumental climate information
- extrapolate instrumental climate information from the regular measuring network to the high elevation ice core sites (including and evaluating short term on site measurements performed during the project)
- collect, homogenize and analyze long-term instrumental climate series and put them at the other groups disposal for the development of climate proxy information

The first two points were covered by the RSC-part of WP-4 ("Recent Site Climatology"), the last by HSC ("Historic Site Climatology"). Some topics like the deduction of lapse-rate series and "precipitation adjusted temperature series" covered both RSC and HSC.

### 3.1. RSC: Recent site climatology

The main objective of RSC was to combine instrumental climate data of the regular meteorological networks of NWSs of the region from the WMO standard reference period 1961-1990 with short term on site or near to site high elevation data, derive adjusting models and thus create regular climate information for the high elevated sites.

#### 3.1.1. Data

RSC Climatology collected data (temperature, precipitation, wind, air pressure, relative humidity and snow depths) from different sources:

Climate data from national and international data holders (METEO FRANCE, METEO SCHWEIZ, Soc. Met. Subalpina Torino, ZAMG, MAP data base) and ALPCLIM meteorological on-site measurements in the Monte Rosa region at Colle del Lys (4236 m asl.) and Seserjoch (4300m asl). Additional data had to be digitised at ZAMG.

#### 3.1.2. Temperature

The vertical distribution of temperature above 1600 asl. was modeled from the regular Alpine climatological network in monthly resolution (for later validation the station of Gr.St. Bernhard was excluded). There is a high correlation between temperature and altitude with  $r^2$  ranging from 0.972 in July up to 0.998 in April. For annual values  $r^2$  was calculated with 0.994. This model can be validated very easily for the Monte Rosa region using the on-site measurements at Colle del Lys for the period 1997-2000. For the region of Mont Blanc the nearest reliable high Alpine measurements are those of Grand St. Bernhard in an altitude of about 2500 m. There is also the high agreement to the vertical model. Taking in account the high correlation of temperature for the two study regions (Böhm et al., 2001) the **vertical temperature model can be applied for the region of Monte Rosa and Mont Blanc.**

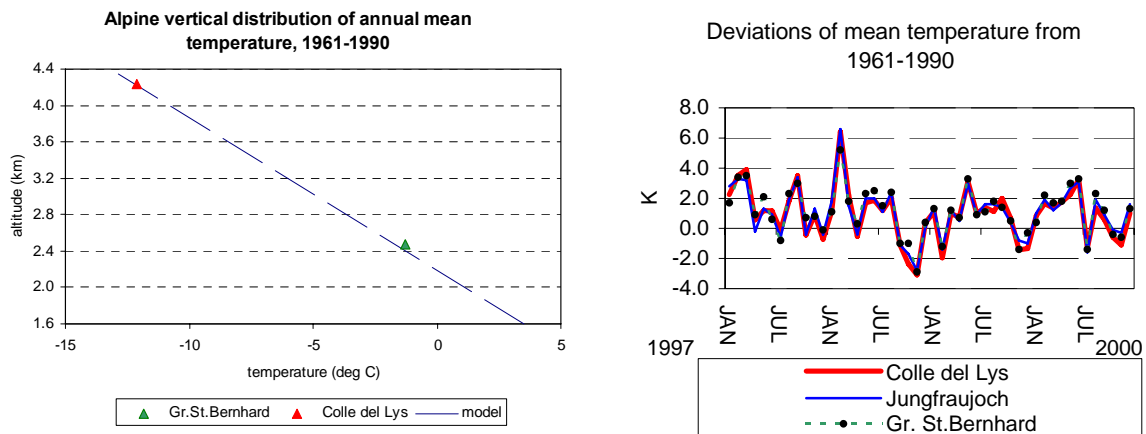


**Fig. 3.1.2.1. Validation of the vertical Alpine temperature model by on-site measurements of Colle del Lys and climate data of Jungfrauoch and Großer St. Bernhard**

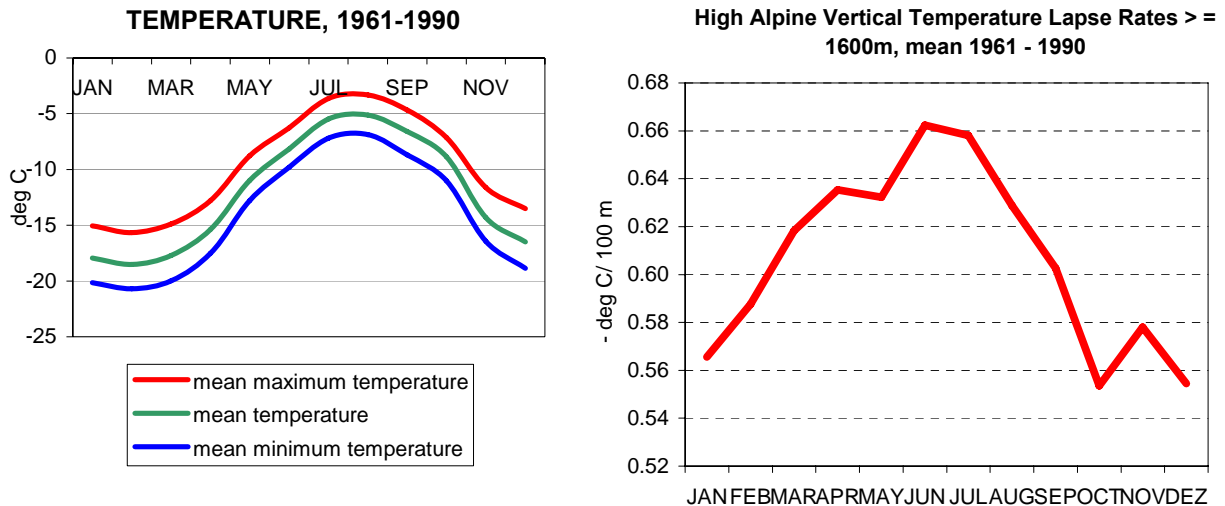


**Figure 3.1.2.2: Annual course of temperature for Colle del Lys and mean lapse rates between 1600 and 4500 asl..**

**Different characteristics of annual temperature course at high and low elevation sites:** The annual course of temperature in the high alpine region shows a characteristic shift of the warmest and coolest months compared to lower elevation sites. In the lower regions the warmest months is July, above 2500 m asl. August is as warm as July, in the 4000 m region August turns out to be warmer than July. There is also a shift from the low elevation coolest month January to February in the high Alpine region. Furthermore the annual amplitude of temperature is decreasing with increasing elevation from around 17 deg K in 1600 m to 13 deg K in 4000 m.

**Vertical lapse rates** reach their maximum between April and July, lowest values occur from October to December.

- The annual course of MDR (**mean daily range**) shows highest values from December to February and lowest in July and August.
- For ALPCLIM purposes the most interesting curves are those of **absolute temperature maximum**. In the elevation of 4500 asl they may exceed the Zero-degree level in July and August.

Mean air temperature belongs to the class of climate elements where the measurements are representative for large regions. The on-site measurements were of exceptionally good quality in respect to the existing weather conditions in 4200 m asl.

### 3.1.3. Precipitation

In contrast to the temperature regime the **characteristics of precipitation are different within the two study regions of Monte Rosa and Mont Blanc**. No on-site measurements are available, moreover some attempts of precipitation measurements in one of the two study regions above 3000 m asl. (undertaken in the Monte Rosa region at Capanna Margherita from mid July till mid September (4554 m asl. 1927-1939 and 1952-1958) and at Plateau Rosa (3480 m asl. since the 1970ies)) are not inspiring at all. The problems of precipitation measurements at high elevation sites are well known and often documented since the beginning of measurements (e.g. Jevson, 1861, Brown et al., 1962, Golubev 1986, Goodison et al., 1989, Auer, 1992 etc.).

In the **Monte Rosa** region the annual course of precipitation sums (Fig. 3.1.3.1.) shows a bi-modal wave with spring (May) and autumn maxima (October). In spring and summer the majority of precipitation events are convective, in winter and autumn advective. In cases of advective precipitation events directions from South are dominating followed by advection from the West. Heavy precipitation events are convective events to more than 50%, in the cases of advective events advection from the South is dominating.

In the region of Mont Blanc the annual amplitude of precipitation amounts is quite smaller, maximum precipitation sums occur in November /December and July/August, minima in April and September. Except summer, the majority of precipitation events are advective ones most pronounced in winter and autumn. The dominating advection comes from West in winter, from South in the other seasons. For higher precipitation events the West direction is dominating.

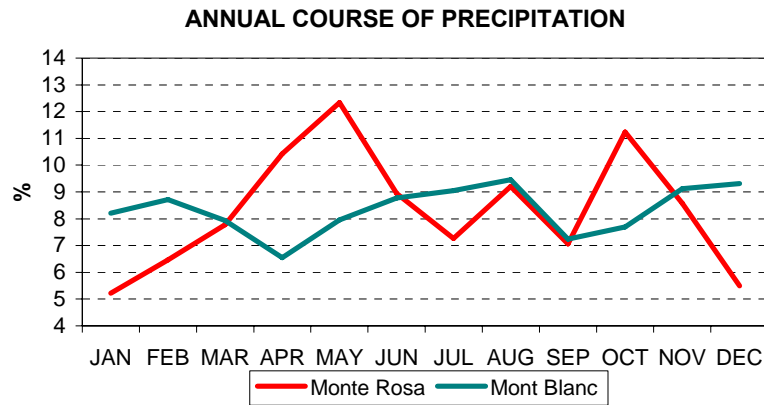
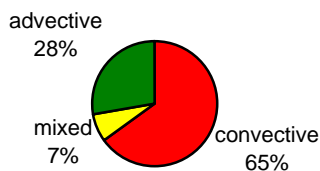


Fig. 3.1.3.1. Mean annual course of precipitation derived for the summit regions of Monte Rosa and Mont Blanc

Percentage of precipitation in the Monte Rosa region in dependence of synoptic weather types, 1961-1990, Summer



Percentage of precipitation in the Monte Rosa region in dependence of synoptic weather types, 1961-1990, Winter

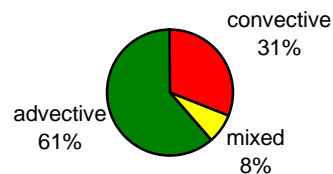
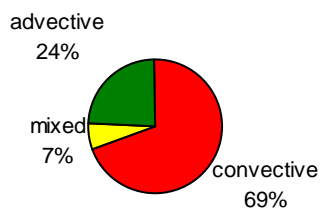


Fig. 3.1.3.2. Mean shares of advective, convective and mixed precipitation in the Monte Rosa region

Percentage of precipitation events in the Mont Blanc region in dependence of synoptic weather types 1961-1990, Summer



Percentage of precipitation events in the Mont Blanc region in dependence of synoptic weather types, 1961-1990, Winter

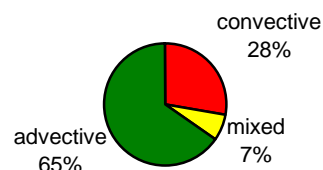


Fig. 3.1.3.3. Mean shares of advective, convective and mixed precipitation in the Monte Blanc region

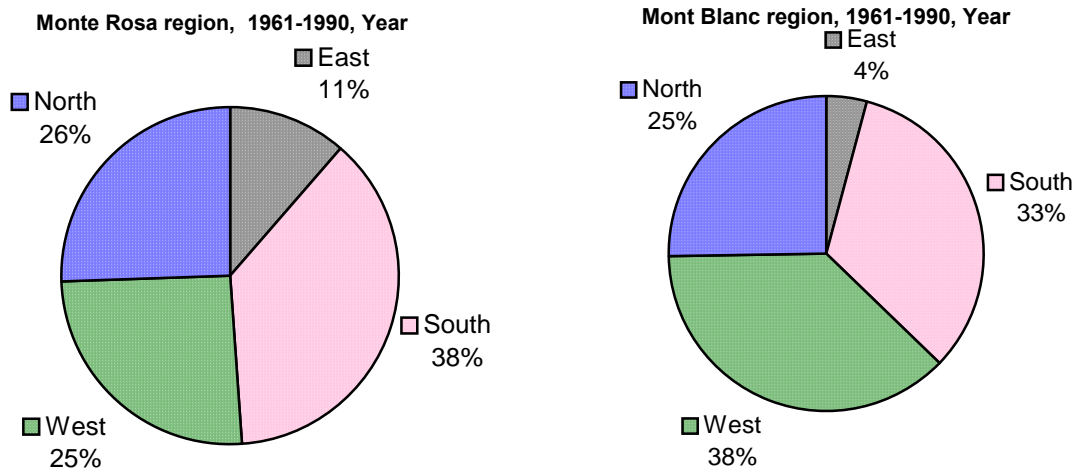


Fig. 3.1.3.4. Mean shares of different directions of advective precipitation in the summit regions of Monte Rosa and Mont Blanc

### 3.1.4. Temperature at Precipitation days

Isotopic data from ice cores are often used as temperature proxies, the isotopic signal in ice cores is directly related to the condensation temperature during the precipitation formation. Climatological temperature series ( $T(\text{CLI})$ ) are calculated from measurements at fixed observation hours throughout the whole year, but ice core temperatures carry the information of temperature during the precipitation events. From long-term temperature series (100 years or longer) this information is not available, what comes nearest to the temperature signal of ice cores in standard climatological data is the temperature of precipitation days weighted by their precipitation amount ( $T(\text{PREC})$ ).

Based on daily temperature and precipitation data, all from stations above 2000 m asl., calculations of monthly values of  $T(\text{PREC})$  been calculated (temperature data on days with precipitation are adjusted due to their precipitation amount), first for all stations separately. A dependence on the altitude of the stations was not found. Further calculations were made using all stations and monthly relationships for the difference  $T(\text{CLI})$  minus  $T(\text{PREC})$  depending on the amount of monthly precipitation were derived by linear regression analyses. These temperature differences showed their minimum from April to July (-0.1 to +0.1 deg C/100% precipitation change) and reached their maximum in November/December (0.4 to 0.5 deg C/100% precipitation change). These “adjusting” values can be applied to long-term temperature series using long-term precipitation series (see HSC-chapter 3.2).

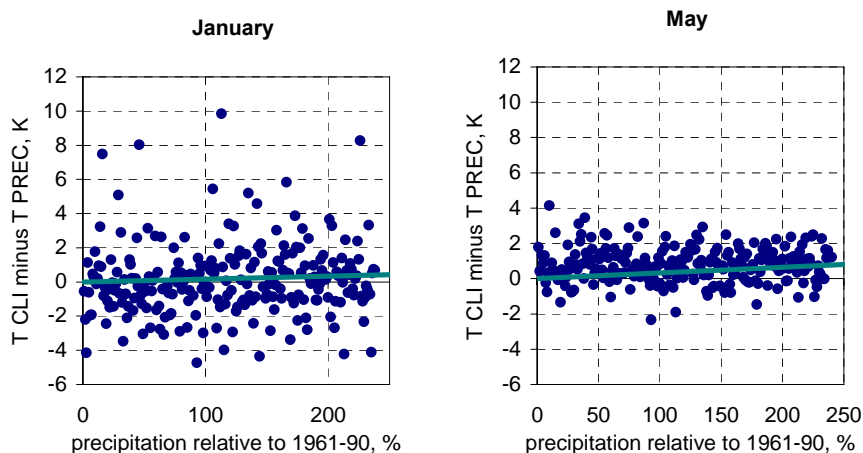


Fig. 3.1.4.1. Examples for scatter plots of differences  $T(\text{CLI})$  minus  $T(\text{PREC})$  versus relative precipitation amounts for the period 1961-1990 in the Monte Rosa region.

The two presented months in Fig. 3.1.4.1 were chosen according to their mean precipitation amounts. May is the month which contributes to more than 10% to the annual precipitation, January only around 6% (for the period 1961-1990). Comparing these two months, it becomes evident, that there is much noise included in these figures anyway, but the variability of “dry” months (like January) is much higher than that of wet ones (like May).

### 3.1.5. Wind

Wind measurements belong to the class of climate elements where the measurements show only local representativity.

#### Wind-roses

The on-site measurements of wind direction are disturbed by orography compared to the free atmosphere. At Colle del Lys wind roses show a distinct maximum from North, only in summer more winds from western directions reduce the North-West maximum. At Seserjoch the most frequent wind directions are Northwest, followed by West-North-West.

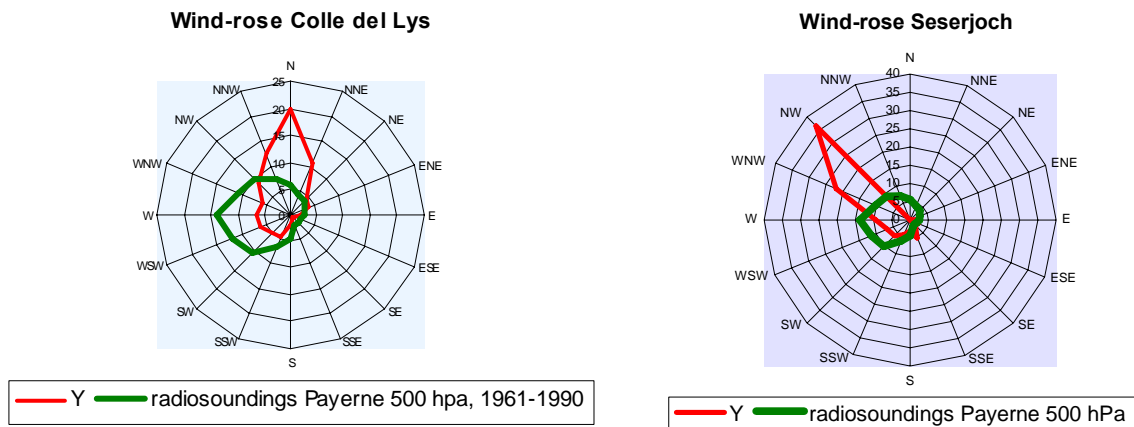


Fig. 3.1.5.1. Mean wind direction distribution for Seserjoch and Colle del Lys (Monte rosa) compared to radio sounding data of Payerne

#### Wind speed

The measured wind speeds turned out to be not exceptionally high within study region of Monte Rosa, but it must be considered that the height of wind sensor was not installed at the WMO standard height of 10 meters. Due to occurrences of freezings of the wind sensor several periods of measurements had to be excluded. So the measurements allow to describe the annual course of wind speed more qualitatively than quantitatively: March is the month with the highest wind speed, around this maximum the period December until April is the windy season with monthly mean values above 6 m/s wind speed. From May until November the monthly mean wind speed stays quite stable around 4.8 m/s.

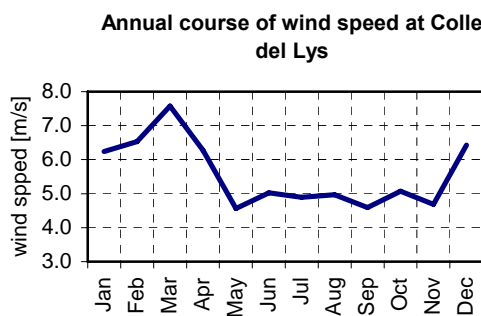
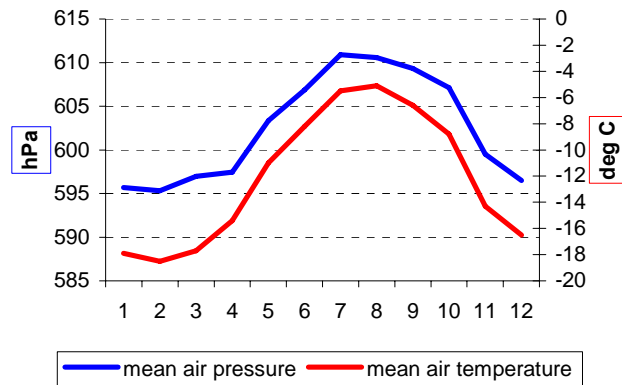


Fig. 3.1.5.2: Annual course of mean wind speed measured at Colle del Lys.

### 3.1.6. Air pressure

Air pressure was modelled and validated by on-site measurements at Colle des Lys. Monthly air pressure reaches in both regions its maximum - depending on the altitude - in July and its minimum in February. The annual course of air pressure and air temperature goes in parallel. The inter-diurnal change of air pressure is lower than 1 hPa for about 50% of days per year.



**Fig. 3.1.6.1. Example for the parallel annual course of air pressure and temperature: Colle del Lys (Monte Rosa), adjusted to 1961-1990 average**

### 3.1.7. Humidity

Relative humidity shows the typical feature for high alpine regions with high values from late spring to summer, and lowest values from September to February. In general the core site altitude band (above 4000m asl.) shows lower relative humidity than the lower regular sites, although Jungfrauoch (3580m asl.) is already close to the +4000m low humidity of the ALPCLIM-sites.

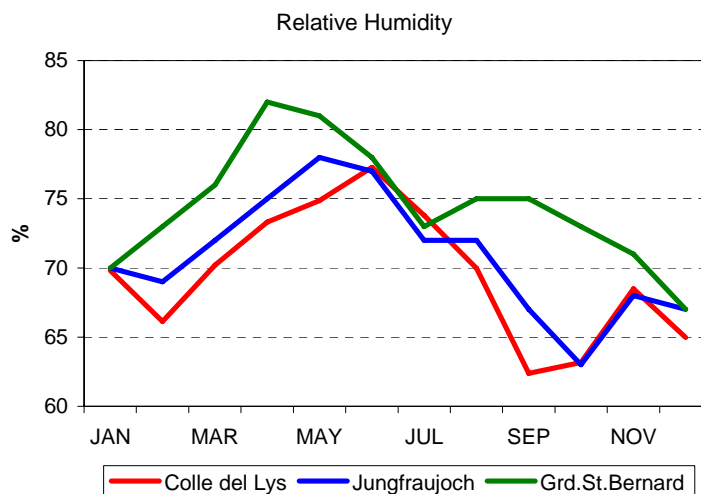


**Fig. 3.1.7.1. Example for the modelled mean annual course of relative humidity for the core site Colle del Lys (Monte Rosa), adjusted to 1961-1990 average compared to the measured climate at the lower altitude sites Grd. St. Bernard and Jungfrauoch**

### 3.1.8 Snow depths and snow accumulation

At Colle del Lys on-site measurements were carried out.

In winter the accumulation rate is very small. On the one hand winter is the season where only 20% of annual precipitation is falling, on the other hand temperatures are the lowest of the year causing smallest particle sizes of precipitation. Winter is also the season with the highest wind speed, so most of the falling snow will be drifted. This means that single months up to one whole winter season can contribute with a loss of snow depths to the annual snow accumulation. Even within one day a considerable loss of snow depths can occur, as it happened on 30 January 1999 with a daily mean wind speed of 20 m/s and a reduction of snow depths of more than 20 cm compared to the day before. If the monthly precipitation rate is high enough like in February 1999, where the Monte Rosa region received more than 250% of normal precipitation rate, snow can accumulate also in winter although the wind speed is not lower than normal. During February 1999 the snow depth increased by 125 cm.

On average spring contributes to snow accumulation, especially May, the months of precipitation maximum and lower wind speed.

Summer contributes to accumulation as well, but even in summer it is not for sure that the falling snow of one single season is stored in the snow pack. Additionally, in summer melting can happen like during the episode from 8.-12 August during the 2 deg K warmer than normal August 1998, when daily temperatures exceeded 0 deg C and snow depth was reduced for about 20 cm.

Autumn (mainly in September and October) offers the best conditions for snow accumulation with the lowest wind speed and higher precipitation rates than in summer.

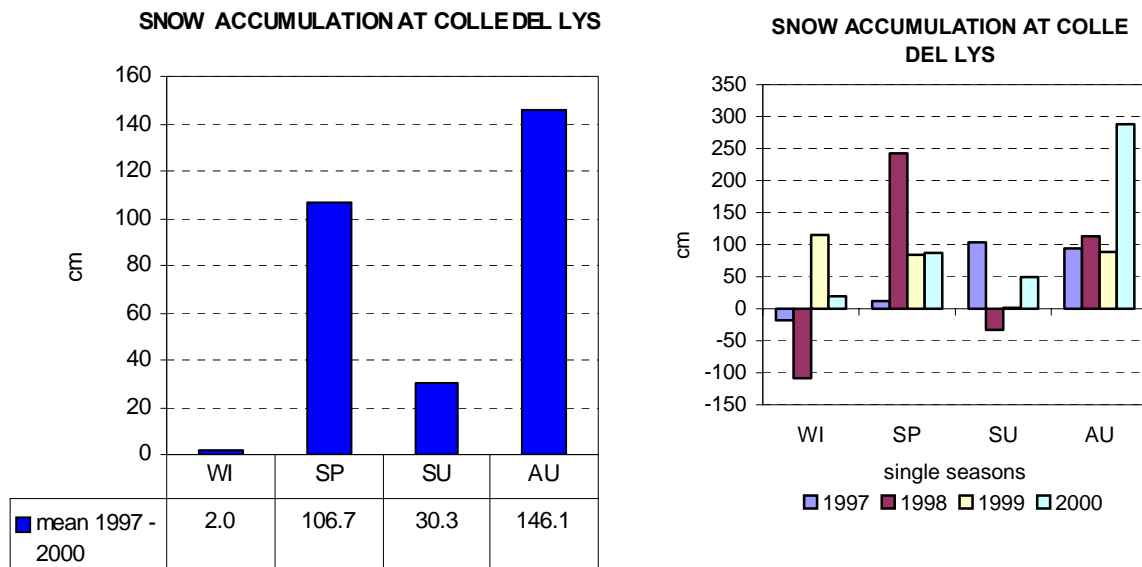


Figure 3.1.8.1: Snow accumulation at Colle del Lys, mean 1997-2000 (left) and single seasons (right).



### 3.1.9 Conclusions

- The on-site measurements at Colle del Lys proved to be very useful. They confirmed the extrapolations derived from the regular climatological networks of NMSs and provided additional on-site information for meteorological elements which could not be extrapolated.
- The calculated statistics of air temperature and air pressure are representative for both study regions, whereas precipitation showed different characteristics.
- Concerning the annual amplitude of temperature there is a shift of the warmest and coolest months compared to lower altitudes, and the annual amplitude is decreasing with increasing height.
- Within the Monte Rosa region there are two distinct maxima in the annual course of precipitation, whereas within the Mont Blanc region the precipitation regime is more balanced during the year.
- Wind and snow data are influenced by regional and local orography, and so only of local representativity.
- In the Monte Rosa region the accumulation season is concentrated to the period between May and October due to the lower wind speeds and higher precipitation rates. In summer shorter periods of melting cannot be excluded.

## 3.2. HSC: Historic site climatology

The main objective of HSC was to produce a high quality instrumental climate data base for the project. As the proxy information from the high elevation ice cores could be expected to cover the climate element temperature mainly, the HSC activities initially concentrated on instrumental temperature data. To study also possible systematic biases of the climate information in the ice cores due to the fact that the “ice core calendar” per definition only stores climate information during precipitation episodes, also precipitation was included into HSC. To enable studies on spatial representativity of the climate information from the ice core sites it became evident quite soon that a spatially extended dataset was desirable. Previous studies in other regions (e.g. Moberg and Alexandersson, 1997) could show that the existing global datasets (Jones, 1994, Jones et al., 1999, Vose et al., 1993, Eischeid et al., 1991, Hulme, 1992, Hulme et al., 1998) have difficulties to meet the quality demands in terms of homogeneity at regional to local scale. A number of studies (Peterson et al, 1998, Auer et al., 2001, Hanssen-Bauer and Nordli, 1998, HMS-WMO 1997 and 1999 among others), could show that strictness in terms of homogeneity is an non negligible precondition for climate variability studies. Non climatological noise in the original series is as large as or larger than the true climate signal. In the Alps there have been some national attempts to homogenize instrumental time series (e.g. Aschwanden et al., 1996, Auer, 1993, Böhm, 1992, Maugeri and Nanni, 1998) but none covered the whole “Greater Alpine Region” (GAR) and some did not use the whole length and spatial density of the instrumental series in the region (which makes the instrumental GAR data potential unique in the world).

Thus the ALPCLIM community decided in the initial phase of the project to carry out a complete re-analysis of the long-term instrumental temperature and precipitation series in a region extending from 4 to 18 deg E and 43 to 49 deg N – understanding “re-analysis” as a collection of all available long-term series to really use the data-potential in the region in terms of length and spatial density, a common and accurate homogeneity check of the series, an elimination of non climatic inhomogeneities and an interpolation to a regular grid to overcome limitations due to inhomogeneities in spatial coverage.

### 3.2.1. Homogenising

All series, original and pre-homogenised, were re-analysed for inhomogeneities based on the following system: homogeneity testing, adjusting and gap-closing was performed in a number of regional sub-groups of 10 series each using the MASH-test of Szentimrey (1999) and the HOCLIS procedure (Auer et al., 1999). HOCLIS (and also the system used by Météo-France, Mestre, 1999) rejects the a priori existence of homogeneous reference series. They test each series against other series in sub-groups of 10 series. The break signals of one series against all other series are then collected in a decision matrix and the breaks are assigned to the single series according to probability. This system also avoids trend imports and an inadmissible adjustment of all series to one or a few “homogeneous reference series”. For temperature high elevated sites (>1500m asl.) were treated separately in two high elevation subregions, for precipitation no homogenisable high elevation series were available due to the well known difficulties of precipitation measuring at high alpine sites which is strongly biased by wind and a high amount of solid precipitation.

Not all of the 120 temperature and 180 precipitation series met the requirements in terms of homogeneity. A final total of 97 temperature and 156 precipitation series proved to be homogenisable.. A total of 1000 breaks were detected in the original, pre-homogenised series. This represents an average of about 4 breaks per series or in other words a homogeneous sub-interval of an average series not longer than approximately thirty years. The availability and the quality of the metadata are different for the different regions and, besides stations with very well documented history, the dataset also contains stations for which only limited metadata were available. As a consequence, it was not possible to perform a complete comparison of the identified inhomogeneities with the history of the stations. It is however, worth noticing that a high percentage of the breaks could be explained through metadata where high quality information was available (for details see Auer et al., 2001).

A comparative analysis of the original and the homogenized temperature series confirmed the necessity of the re-analysis in terms of homogeneity. Fig.3.2.1 shows the mean difference series of all ALPCLIM temperature series (homogenized minus original). There is not only a large range of inhomogeneities in the single series ranging from minus 4 to plus 3 K – also the average of all adjustments (the bold line) is not zero (as it should be if all inhomogeneities were non systematic) but

shows a systematic bias of an under-estimation of the long term temperature trend in the region by the original series of 0.5K.

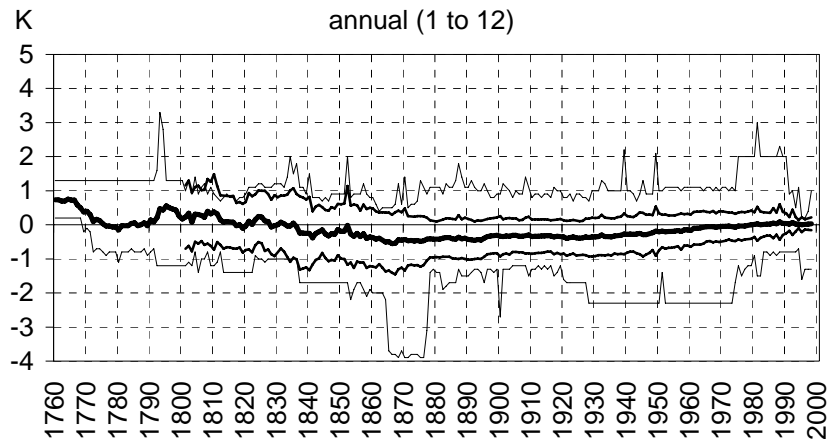


**Fig. 3.2.1. Long-term adjustment curves (homogenised minus original) averaged over all 97 ALPCLIM sites for the annual temperature series**  
**Bold line: mean, medium lines: standard deviation range, thin lines: absolute range.**

An additional comparison with the respective grid boxes of the widely used CRU-gridded temperature dataset (CRU = Climatic Research Unit of the University of East Anglia, Jones, 1994, Jones et al., 1999) confirmed the initial reservations against the use of non homogenized data and the usability of global datasets in regional scale. It is clear to see that also the CRU-series are systematically biased versus the homogenized ALPCLIM-series by 0.6 to 0.8K. The bias is even slightly stronger than the one of the homogenized versus the original ALPCLIM series.

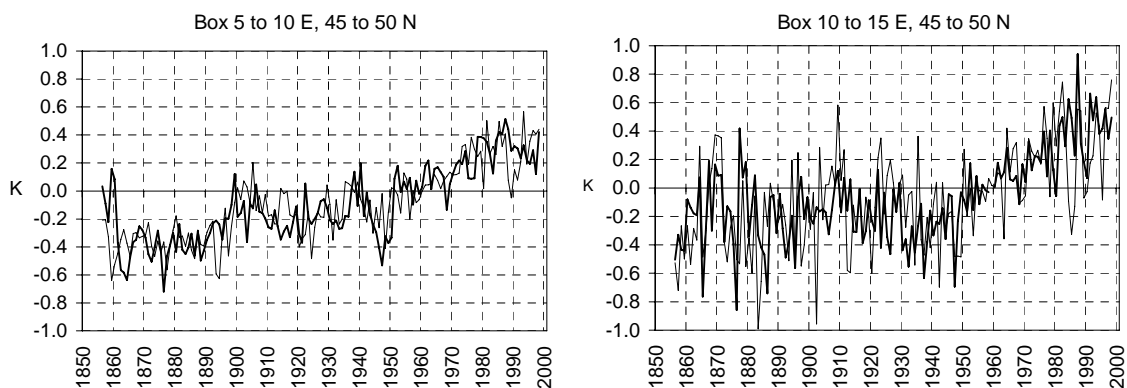


**Fig. 3.2.2. Difference series of temperature (ALPCLIM minus CRU) 1856 to 1998 for the two grid boxes with 83% common coverage. Both relative to 20<sup>th</sup> century mean, bold: summer half year (months 4 to 9) thin: winter half year (months 10 to 3).**

As already mentioned there are good reasons to believe that the ALPCLIM data are nearer to the real climate than the CRU data. A comparison with another Alpine temperature time series developed by Böhm et al., 1998 may serve as another argument in favour of ALPCLIM. This is a temperature time series derived from air pressure series of a number of high-level and low-level sites in the Alps. Without going into details (these are given in the mentioned reference) the authors of the study used the fact that the warming of an air column between a low-level and a high-level site must produce a decreasing difference of low-level versus high-level air pressure due to thermal expansion of the air between. In fact, it is not the difference but a logarithmic ratio based on the barometric height formula, and it is not temperature but virtual temperature – but the latter could be shown to be negligible. The result is clear, the independent modelled temperature series strongly support the credibility of the ALPCLIM data with a twice as strong centennial trend as the CRU trend.

Concerning the precipitation homogenisation similar comparisons homogenised minus original and ALPCLIM versus large scale datasets have not been done yet. The share of already pre-homogenised series was higher than for temperature and the “original” database in the ALPCLIM-region was therefore not reconstructable. For parts of the study region (the eastern Alps) Auer et al., 2001 could

show that also the original precipitation series are strongly biased by non climatic noise. A comparison with the gridded global land precipitation dataset of CRU (Hulme, 1992, Hulme et al., 1998) is in work and will be published in the planned ALPCLIM precipitation publication mentioned above. The global CRU dataset covers the period 1901-1998 and is available in two spatial resolutions (5x5deg and 2.5x3.75deg). Thus the homogenised high density ALPCLIM precipitation dataset – covering the last two centuries in 1x1deg resolution - is a novelty in climate time series research.

### 3.2.2. Gridding

For easier and more systematic mathematical handling, and to enable a comparison with other gridded datasets, the single series were interpolated to grid points. The idea behind gridding was not a further data compression, but more a shifting of information to equidistant points. The ratio of single series to the number of grid points is not far from one at the chosen grid spacing of 1 deg longitude and latitude. Interpolation was performed by a Gauss-weighting function with weight 1 at the location of the grid point and quickly decreasing to 0.1 at 200km distance. In principle, all single series contribute to each grid point but at very small weights at larger distances from the grid point. To avoid large distance information transport in cases where no series exist near the grid point (this is typical for the older parts of the series with sparse spatial resolution), interpolation was truncated at the starting year of the longest single series within 200km distance from a grid point. Taking into consideration some existing steep climate borders within the study region (as for example the main alpine divide, coastal versus inland regions, regions with different annual course of precipitation and others) some such sub-regions were defined among which no information exchange was allowed. Figs. 3.2.3. and 3.2.4. show those sub-regions (for temperature and for precipitation).

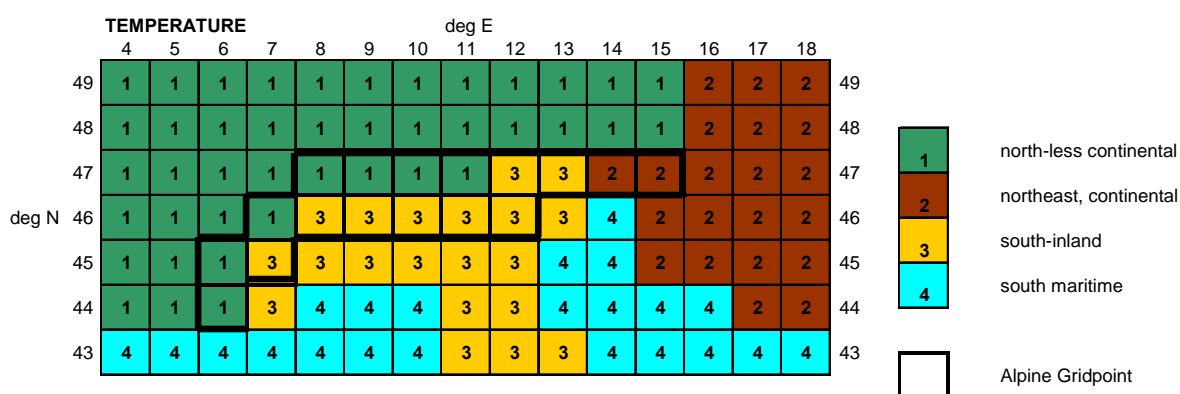


Fig. 3.2.3. Climatologically different sub-regions with no information exchange in gridding – temperature

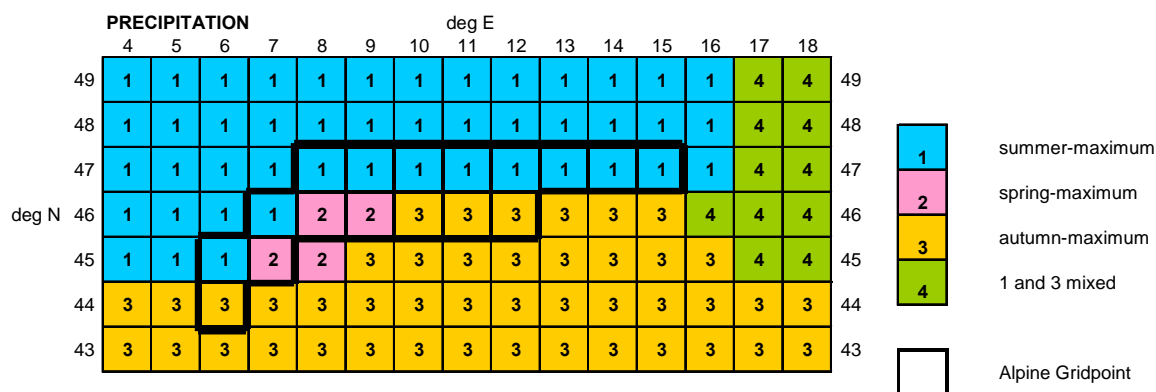


Fig. 3.2.4. Climatologically different sub-regions with no information exchange in gridding – precipitation

### 3.2.3. The gridded datasets

The main deliverable of HSC are the new homogenized and gridded ALPCLIM datasets of temperature and precipitation. They consist of gridpoint series on a 1x1-deg grid. All series are monthly series relative to the 20<sup>th</sup> century mean (subtractive for temperature, ratios for precipitation).

For temperature two grids in different sealevels have been generated, the precipitation grid refers to altitudes below 2000m asl only (due to the already mentioned difficulties concerning high elevation precipitation measurement). Fig. 3.2.5 shows the starting years of each grid-point series. Large areas of the study region are covered by more than bi-centennial temperature series, the longest starting as early as 1760. The high-elevation temperature grid starts between 1818 (western Alps) and 1851 (estern Alps). The typical starting period of the precipitation grid is the first part of the 19<sup>th</sup> century, the longest series start in 1803.

In addition to the systematic homogenization it is the length of the instrumental grid-series mainly that makes them a unique new tool for any kind of climate analysis within the project and also for research groups outside the project. One of many fields of research may be mentioned here – glaciology. Glaciological research in the Alps can rely now not only on new temperature series but also on precipitation series starting as early as in the first part of the 19<sup>th</sup> century, the period of the last and one of the strongest glacier advances in the Holocene. Within the project the dataset was used for comparison with the proxy information derived from stable water isotopes of the project’s ice core sites (section 3.2.4.3).

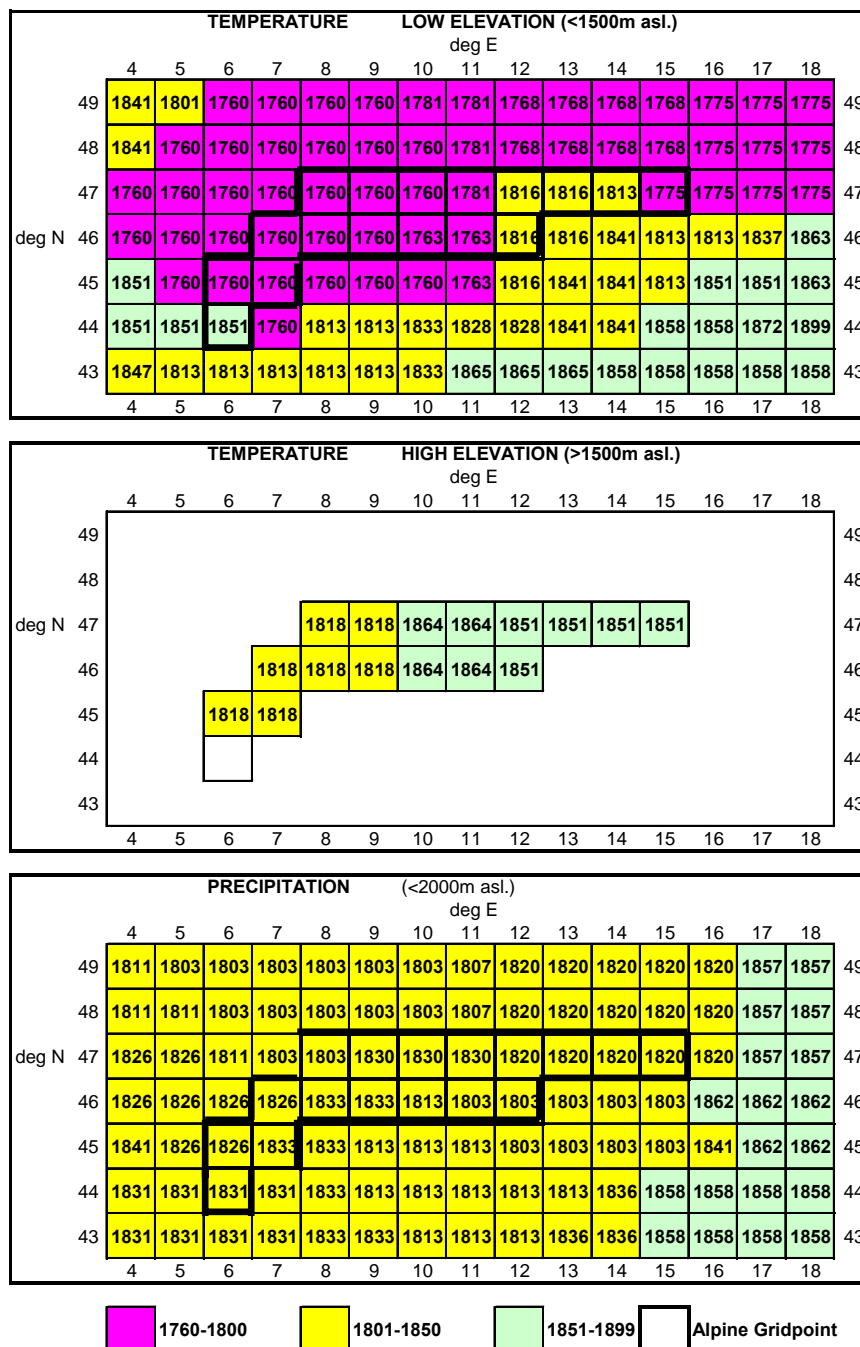


Fig. 3.2.5. Starting years of the new homogenised and gridded ALPCLIM datasets

### 3.2.4. First analyses of the new datasets

The ALPCLIM temperature dataset has been analyzed already and published (Böhm et al., 2001). A similar analysis of the precipitation dataset is in work and will be published in the same journal. Examples of both analyses are shown here.

#### 3.2.4.1. Instrumental temperature variability in the greater Alpine region (GAR) since 1760

A principal component analysis (PCA) based on the monthly series (VARIMAX rotation according to Richman, 1986) allowed a clustering of the GAR temperature data into six sub-regions (five horizontal ones and one vertical, compare Fig.3.2.6). This PCA-regionalisation corresponds to the high frequency variability and does not necessarily reflect different long-term variability in the sub-regions. A comparative trend analysis in fact showed, that the long-term temperature evolution in the instrumental period is rather uniform in the entire GAR (Fig.3.2.7). Also the smoothed high-elevation variability (the dark blue curve in Fig.3.2.7) is highly similar to the low elevation regional curves. Therefore – if only the long-term features are of interest – not only the high-elevation subgroup can be used for comparison with the proxy information from the high elevation ice cores, but also the (longer) low elevation subgroups or even the mean over the entire GAR.

The length of the ALPCLIM series enables an analysis of data covering the “pre-industrial” period, which is frequently used for comparison with the warmer (most likely already anthropogenically influenced) 20<sup>th</sup> century climate. For global datasets, data coverage limits the length to starting points not earlier than the mid-19<sup>th</sup> century. In the Alps and their surroundings, there are another 90 years of instrumental temperature information prior to 1850. This changes the results of trend analysis because the early period is not characterised by low temperatures but shows high temperatures especially in spring and summer.

The annual data (Fig.3.2.7) show a start from lower values before 1785, followed by two relative maxima in the 1790s and the 1820s, interrupted by a sudden cold event in the 1810s. After the 1820s there is a gradual trend towards two minima in the 1840s and 1850s and the 1880s and 1890s with a relative maximum in the 1860s and early 1870s. The whole 20<sup>th</sup> century is characterised by rising temperature towards a first maximum near 1950 and a second in the 1990s, which is the main maximum of the 240 ALPCLIM years. Compared to the global mean temperature evolution (the black curve in Fig.3.2.7) temperature increase in the Alps since the late 19<sup>th</sup> century has been significantly stronger.

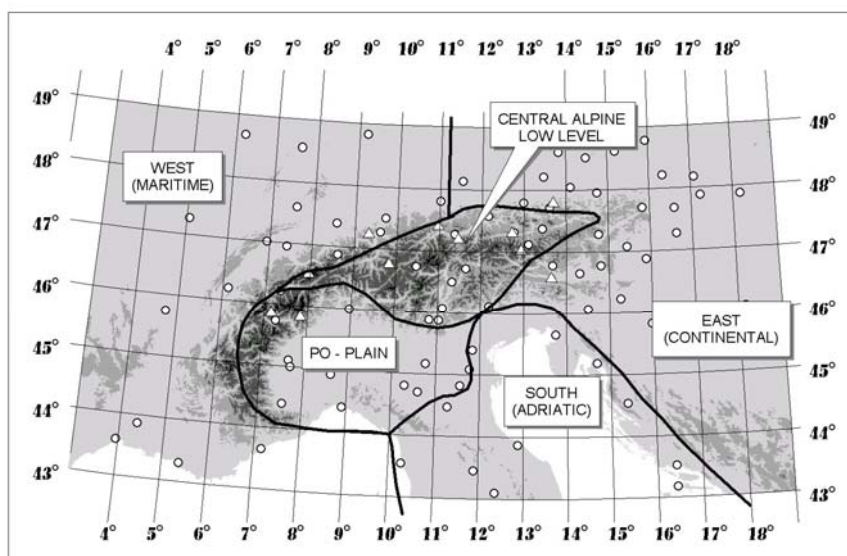
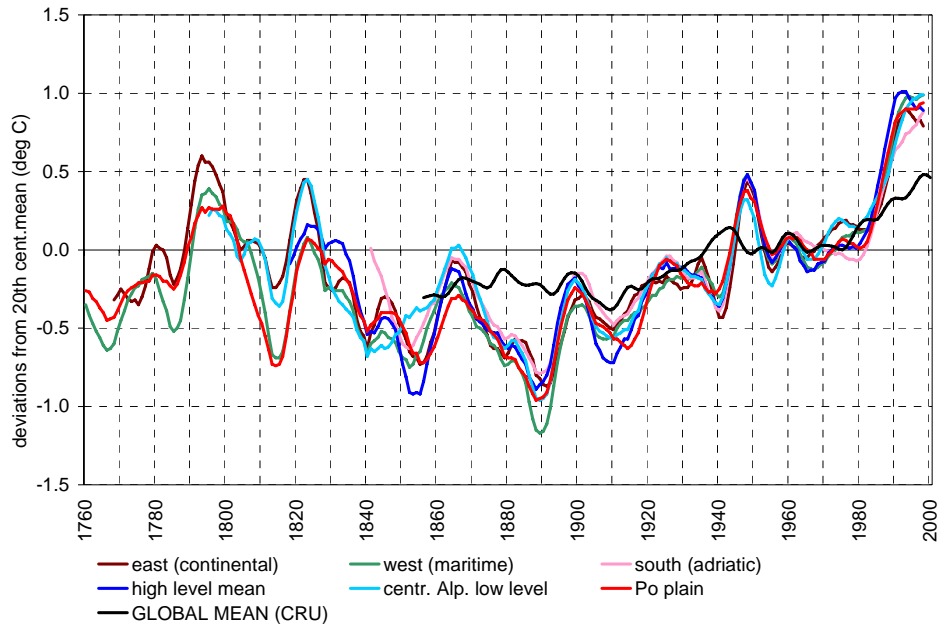
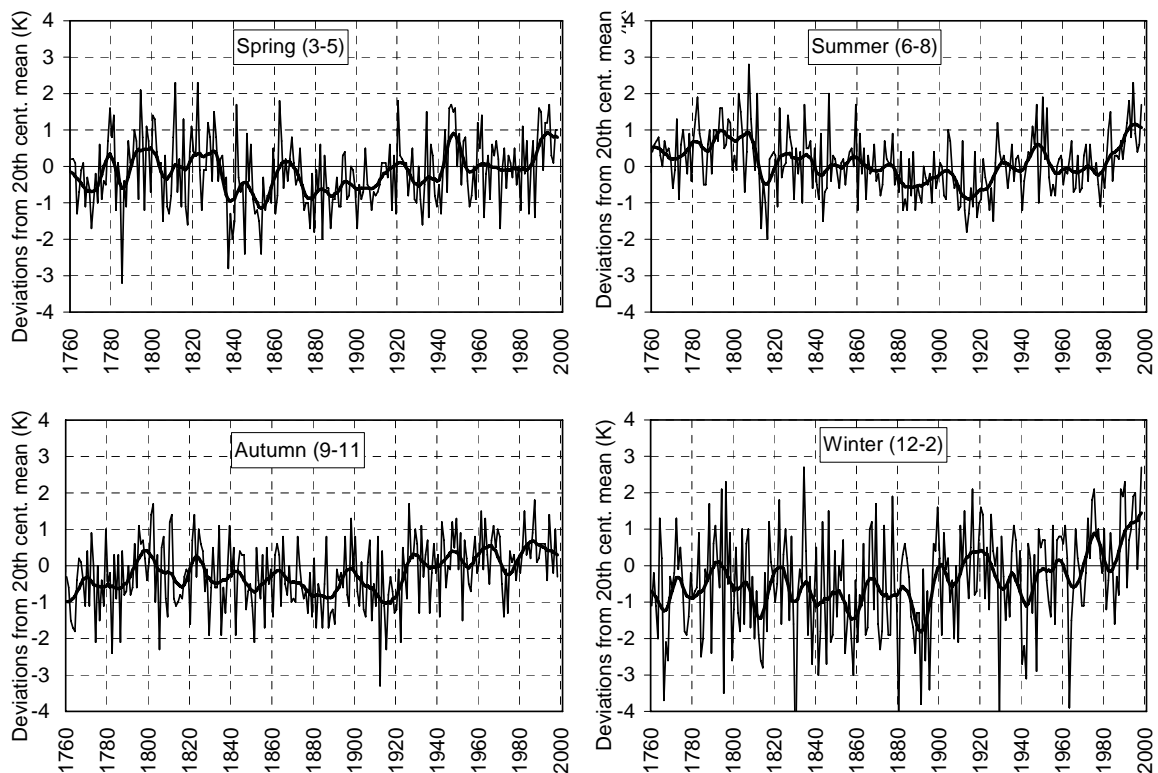


Fig. 3.2.6. Map of temperature sub-regions based on Principal Component Analysis clustering



**Fig. 3.2.7. Annual mean sub-regional temperature series in the greater Alpine region (GAR) (deviations in K from 20<sup>th</sup> century mean) smoothed with a  $3\sigma$  gaussian low pass filter (11 years wide running window).**

The analysis of the seasonal temperature series (Fig. 3.2.8.) gives evidence for strong seasonal differences. Concentrating on the long-term features alone, annual and seasonal mean GAR series initially decrease to a minimum, which is then followed by a positive trend until 1998. The location of the minima is different however, 1890 for the entire year and winter, 1840 for spring and 1920 for summer and autumn. The initial decreasing trend is more evident in spring and summer, less in autumn and smallest in winter



**Fig. 3.2.8. Seasonal mean temperature series in the greater Alpine region (mean over entire GAR) single years and smoothed with a  $3\sigma$  Gaussian low pass filter (11 years wide running window).**

### 3.2.4.2. Instrumental precipitation variability in the greater Alpine region (GAR) since 1803

Unlike temperature with highly similar long-term variability in the entire study region, precipitation shows considerable spatial differences according to seasonal mean features as well as according to short-term and long-term variability.

Figs. 3.2.9 and 3.2.10 show the regionally different mean annual courses of precipitation in the GAR. The main climatic divide is the Alps with a prevailing Summer maximum north of the Alps and a bimodal annual course in the south. The latter can be sub-divided into three groups – one in Piedmont with the main maximum in Spring, one in the central and eastern south with the main maximum in Autumn and one in the southwest and southeast with an Autumn maximum and very low summer precipitation. The fifth group in the north-east shows a summer maximum and an additional weak Autumn maximum.

In the dataset each grid-point series (consisting of relative monthly precipitations as ratios of the 20<sup>th</sup> century mean) is accompanied by the mean relative share of each month on the annual total. This enables the user to calculate any seasonal or annual mean series using that information for calculating the weighted averages.

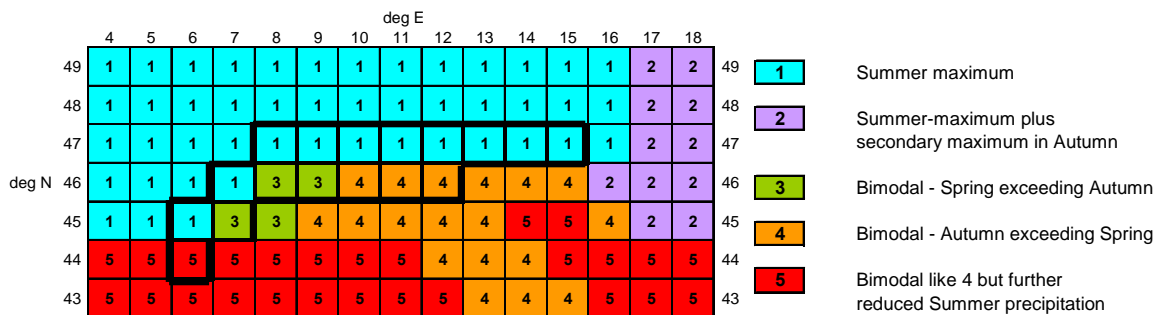


Fig. 3.2.9. Regionalisation of the study region according to mean annual course of precipitation

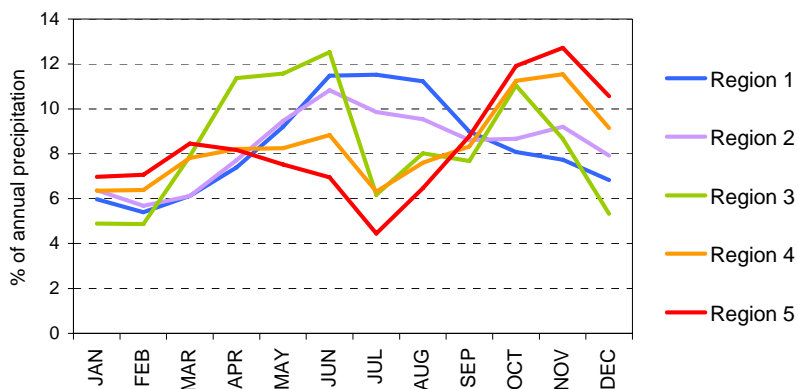


Fig. 3.2.10. Mean annual course of precipitation in the sub-regions of Fig. 3.2.9

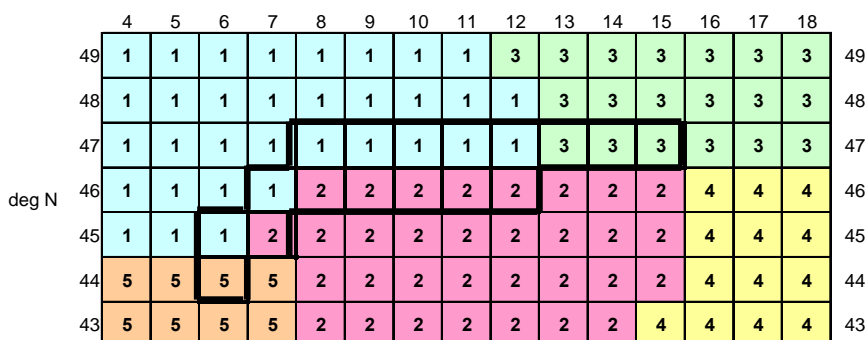
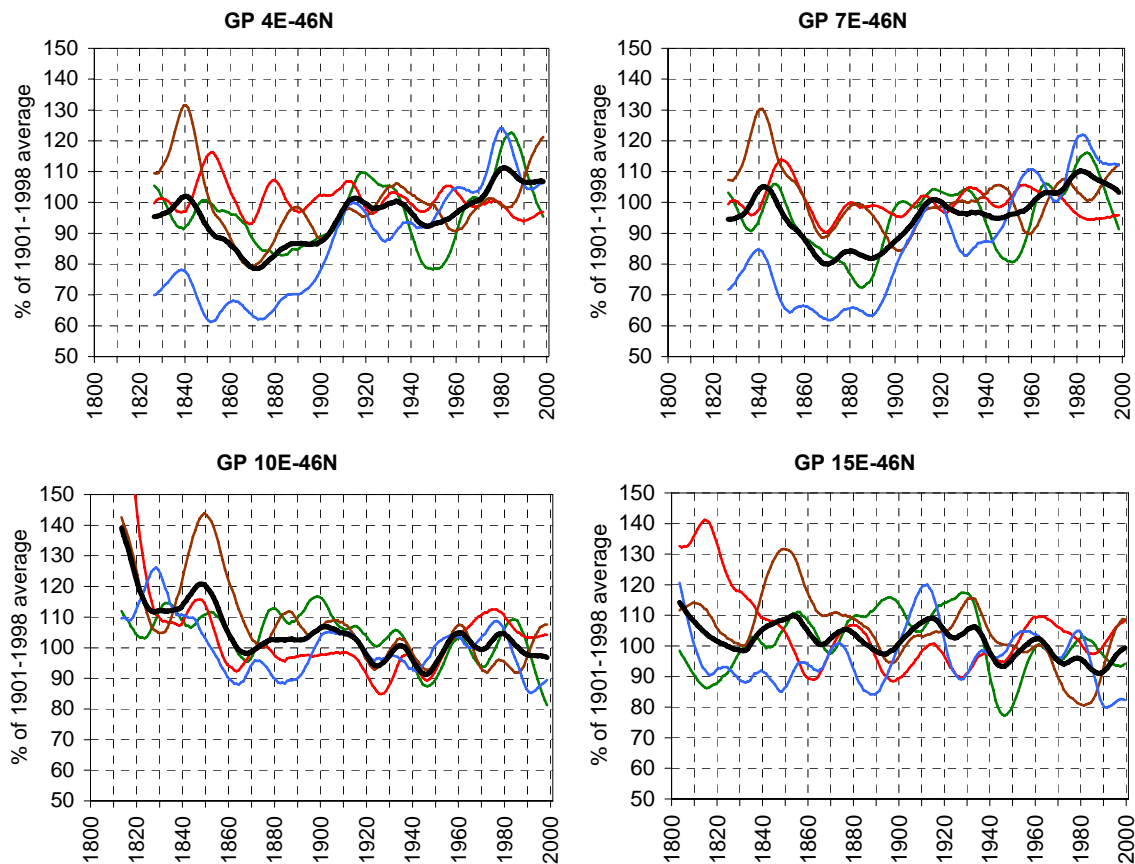


Fig. 3.2.11. Map of precipitation sub-regions based on Principal Component Analysis clustering



A regionalisation in respect to variability patterns was carried out based on the same way of proceeding as for temperature – using a principal component analysis for clustering (Fig.3.2.11). The result is similar but not identical to the regionalisation based on mean annual course. Again the Alps are the main divide. The second variability structure is a meridional one – sub-dividing the region north of the Alps in a western and an eastern part, whereas south of the Alps three sub-regions could be identified.

As already discussed in section 3.2.4.1 PCA clustering reflects short term variability rather than long-term variability and does not necessarily mean that the long-term evolutions in the spatial sub-regions are different. For temperature they are not (compare section 3.2.4.1) – the long-term variability is highly similar in each sub-region of the GAR. Precipitation is different - there are no long-term features which are representative for the whole study region. Long-term precipitation variability shows a number of different evolutions – some examples are shown in Fig. 3.2.12. and Fig. 3.2.13.



**Fig. 3.2.12. Smoothed annual and seasonal precipitation grid-point series in the GAR: Cross-section along 46<sup>th</sup>N-parallel. (30-years Gauss low pass filter; bold black: annual, green: Spring, red: Summer, brown: Autumn, blue: Winter; all values relative to 1901-1998 average)**

The two figures show cross-sections through the study region, one along the 46<sup>th</sup> N parallel and one along the 12<sup>th</sup> E meridian – the first crossing the western Alps (between 7 and 10 deg E), the latter crossing the eastern Alps (between 48 and 46 deg N). In both cases the main Alpine divide acts as a sharp climatic trend between long-term generally increasing precipitation west and north of the Alps versus a general decreasing trend south and east of the Alps at least during the last 120 years. The early parts of the series (before 1850) show high precipitation amounts in all sub-regions. The increasing trends are strongest in winter, weakest to non existing in summer, the decreasing trends in the south are strongest in summer, less pronounced in the other seasons, weakest in winter. The long-term trends are not homogeneous – there are a number of superposed shorter oscillations on decadal scale, not only in the shown examples, but in the whole dataset.

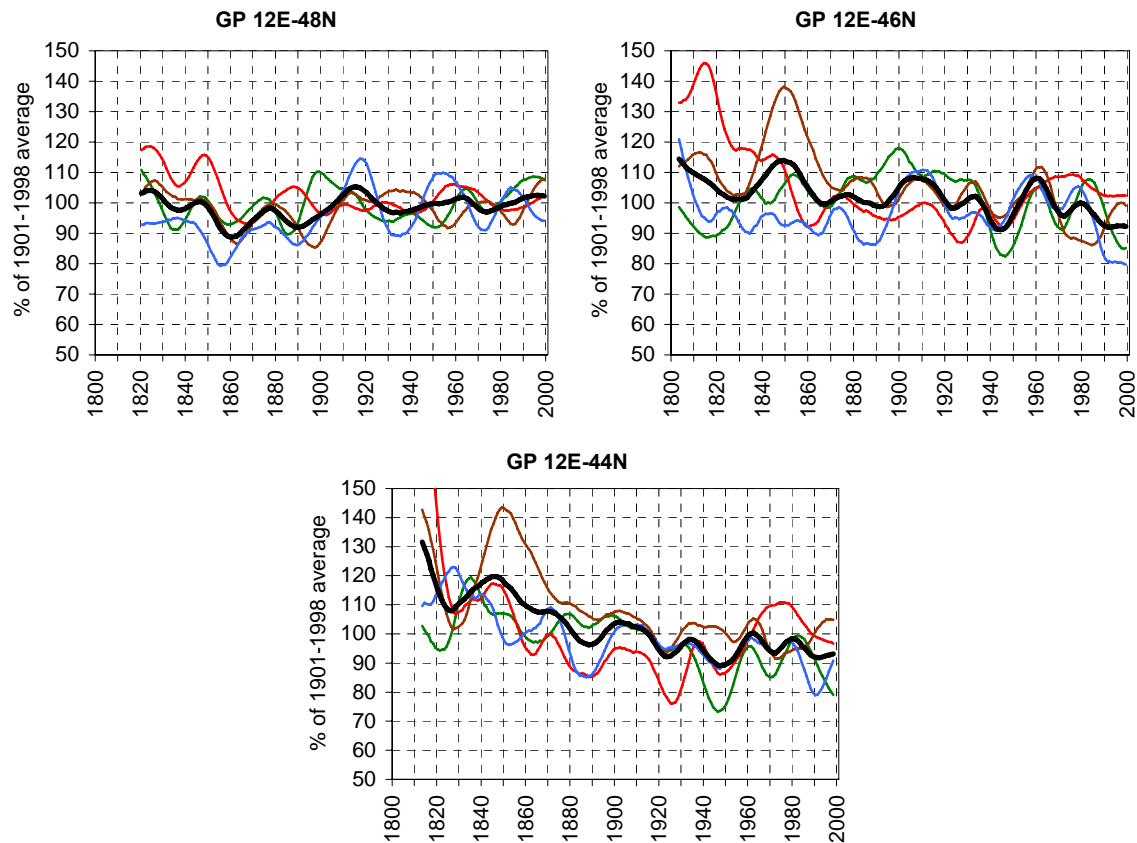


**Fig. 3.2.13. Smoothed annual and seasonal precipitation grid-point series in the GAR: Cross-section along 12<sup>th</sup>E-meridian. (30-years Gauss low pass filter; bold black: annual, green: Spring, red: Summer, brown: Autumn, blue: Winter; all values relative to 1901-1998 average)**

An overview on the spatial patterns of annual precipitation variability in the entire study region at a one deg longitude latitude resolution is given in Figs. 3.2.14. and 3.2.15. The figures display each grid-point's decadal mean precipitation deviation from the 20<sup>th</sup> century average of the respective grid point, the strength of the deviation is given by a color code ranging from less than 80% to more than 120%. The bold framed grid-cells show the position of the Alps.

Although the first decades of the 19<sup>th</sup> century have no complete data coverage, they are important anyway because there has not been any reasonable and high quality precipitation information from systematically homogenized and gridded instrumental series in the Alps so far. They will supply e.g. the glaciological community with new information to explain the extraordinarily strong glacier advances before 1850, which have not been easy to explain by temperature alone. The first part of the 19<sup>th</sup> century seems to have been a period with the highest precipitation amounts in most parts of the study region – the center of precipitation activity slowly shifting from the NW to SE during those early 50 years of the instrumental period. With increasing spatial data coverage towards the mid-19<sup>th</sup> century a dipole-like structure with two centers in the NW and in the SE emerges more and more clearly which keeps on to be the prominent feature of precipitation variability in the GAR throughout the whole instrumental period. This dipole structure is in accordance to the first two principal components of the PCA-analysis mentioned before. It remains in the first mode (wet in the SE, dry in the NW) throughout the whole 19<sup>th</sup> century and in the first decade of the 20<sup>th</sup> century – the drying of the NW being most pronounced in the 1860s, 70s and 80s (and moving from the NE to the SW in those three decades). The high-precipitation cell in the south is strongest in the first part of the 19<sup>th</sup> century and weakens and moves to the east in the second part of the 19<sup>th</sup> century.

In the 20<sup>th</sup> century (Fig.3.2.15) the spatial differences are generally less pronounced than in the 19<sup>th</sup> century but the dipole-structure keeps on to exist. Only in the 1910s it nearly breaks down (moderately high precipitation in the whole study region, only weak regional differences) and the spatial pattern starts to re-emerge during the following decades in a reverse mode to the previous century – the South begins to dry out and the NW starts to receive more and more precipitation. The drying of the South starts earlier (clearly visible in the 1920s already), whereas the increasing precipitation in the NE is strongest in the second part of the 20<sup>th</sup> century.

### 19<sup>th</sup> CENTURY

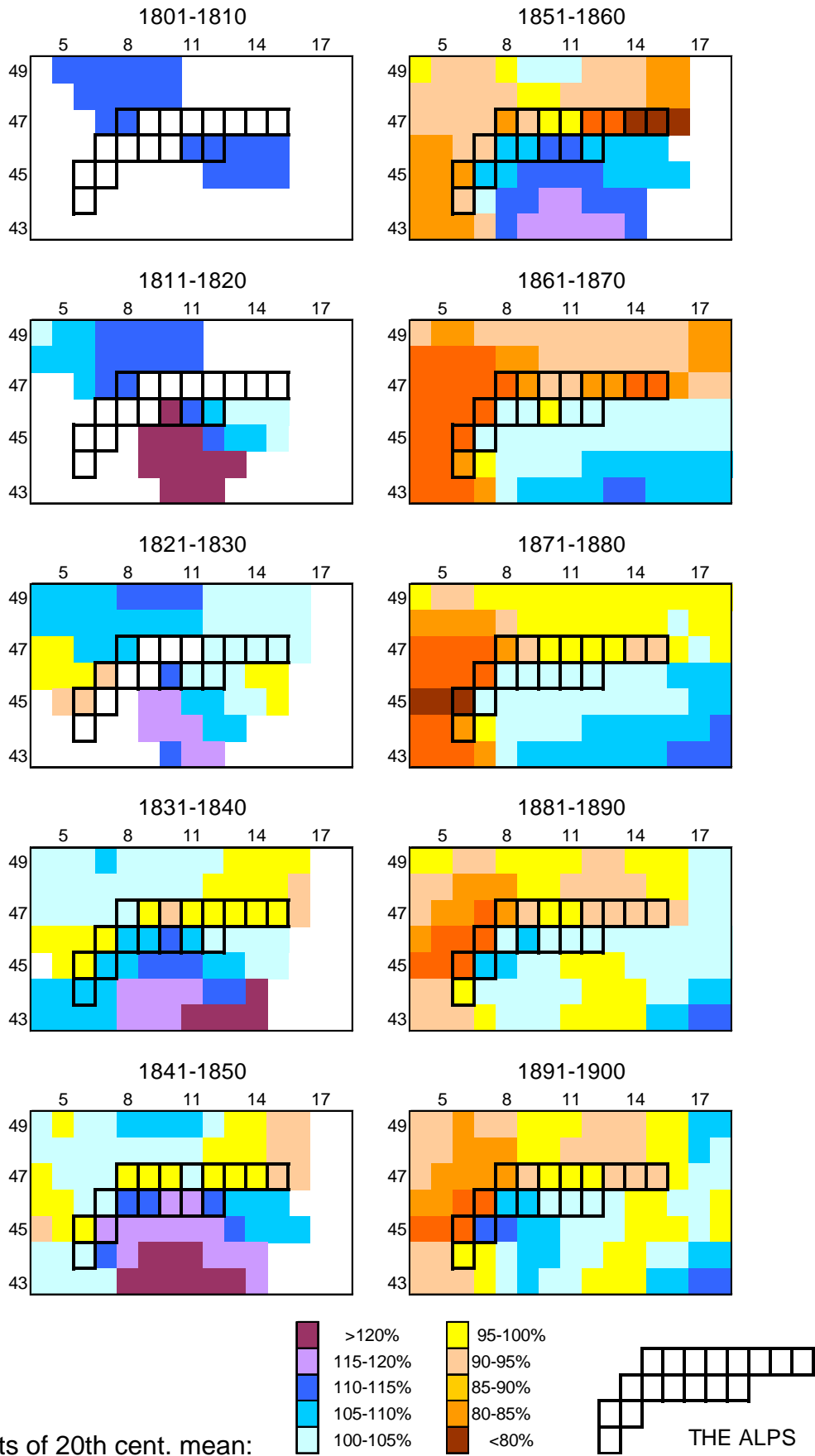


Fig. 3.2.14. Spatial patterns of decadal mean precipitation variability in the greater alpine region in the 19<sup>th</sup> century.

### 20<sup>th</sup> CENTURY

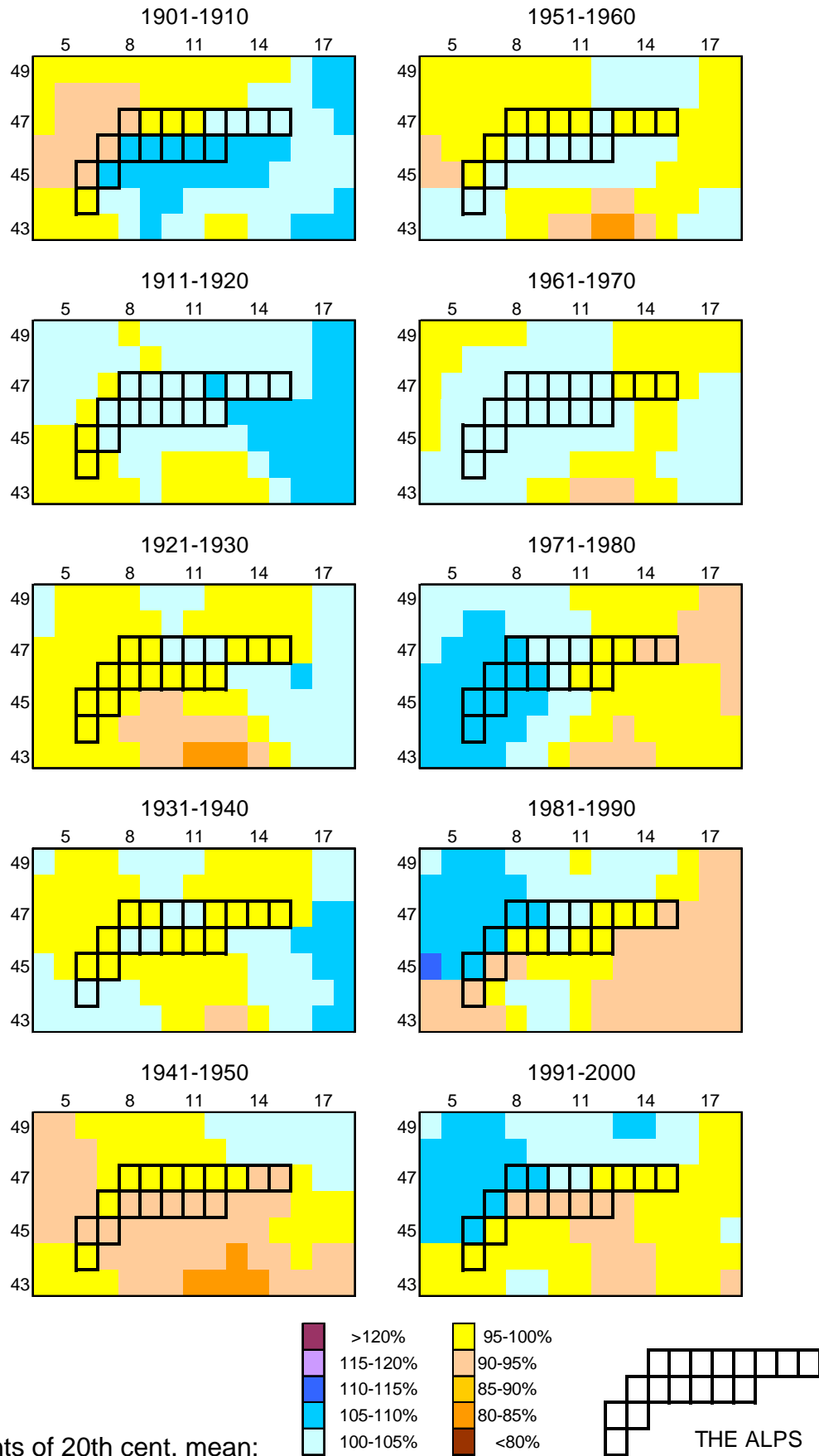
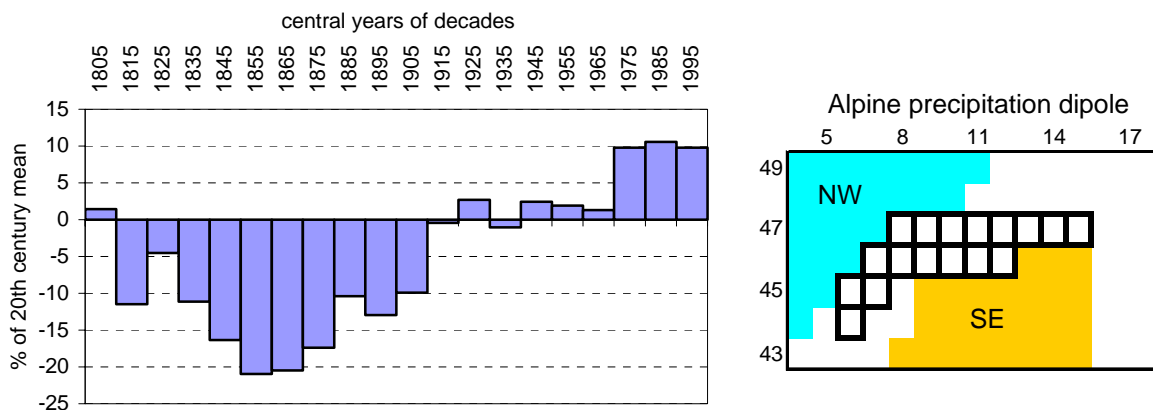


Fig. 3.2.15. Spatial patterns of decadal mean precipitation variability in the greater alpine region in the 20<sup>th</sup> century

One feature of the precipitation variability patterns in the GAR – the NW-SE-dipole – is becomes clearer in the difference time series of the NW- versus the SE-average precipitation shown in Fig.3.2.16. The conversion from a fully developed mode-1 (SE>NW) in the 19<sup>th</sup> century developed quite regularly and smoothly over a long conversion period in the first part of the 20<sup>th</sup> century with no dipole-structure to a fully developed mode-2 (NW>SE) in the latest 3 decades of the 20<sup>th</sup> century.



**Fig. 3.2.16. Left: Time series (months 1-12) of the precipitation differences NW minus SE (the centers of the “Alpine precipitation dipole”) – both relative to 20<sup>th</sup> century mean  
Right: grid-points used for the calculation of the subregional means NW and SE**

This “Alpine seesaw” is obviously caused by circulation changes together with the influence of the Alpine topography on precipitation. A planned follow-up study is going to study and explain that prominent climate feature in the GAR using high resolution regional climate modeling (Böhm et al., 2001). Taking into account the geographical position of the two ALPCLIM ice core sites in the summit regions of Mont Blanc and Monte Rosa – the first exposed towards NW, the latter towards SE – it can be assumed right now that in times of a fully developed dipole structure the two sites might be under rather different influence concerning the source regions of precipitation (Atlantic for Mont Blanc, Mediterranean for Monte Rosa) whereas in times of a weak dipole structure (e.g. the decades from 1910 to 1960) the splitting into different source regions should be less important for the two sites.

### 3.2.4.3. Spatial representativity of Alpine temperature series for Europe

As one of the results of project ALPCLIM are proxy temperature series derived from stable water isotopes from high elevated ice core sites in the summit region of Monte Rosa (chapter a), it is interesting to study the question for what area temperature information from high elevated sites (more than 4000m asl.) is representative. Schöner et al., 2001 analysed the spatial correlation of the ALPCLIM instrumental high elevation temperature grid point series 8E-46N with the gridded temperature dataset of CRU (Jones, 1994, Jones et al., 1999). The analysis was performed for summer half-year (months 4 to 9) and winter half-year separately in order to take into account the different vertical temperature lapse rates in summer and winter which should produce a stronger isolation of high elevated alpine sites in winter and a closer correlation of them with low elevation Europe in summer.

The two correlation maps of Fig.3.2.17 show the spatial distribution of the summer (a) and winter (b) correlation of the high elevation grid-point temperature of the Monte Rosa summit region with the rest of Europe. In summer the high-elevation temperature information from the highest alpine summits is significantly correlated (at the 99% significance level) with a large part of Europe represented by a circle around the 8E-46N grid-point of approximately 10deg radius. Very high correlation (>0.6) is given for most of Central Europe and the western Mediterranean from western France to Hungary, northern Germany to northern Algeria. Regions of negative correlation are as far away in summer as Iceland in the northwest and Egypt in the southeast. In winter the shape of the correlated region changes to a more SE-NE-orientated ellipse, the highly correlated regions (>0.6) are strongly reduced and show a clear orientation towards the Atlantic. Correlations >0.8 exist in summer only and only for a small region in the western and parts of the eastern Alps. In winter the high elevation Alpine summits are de-coupled from the low elevation lowlands by the frequently occurring stable and cold low elevation air-masses, whereas the high summits are closer linked to advection from the Atlantic which does not penetrate too often into the low elevation surface layers.

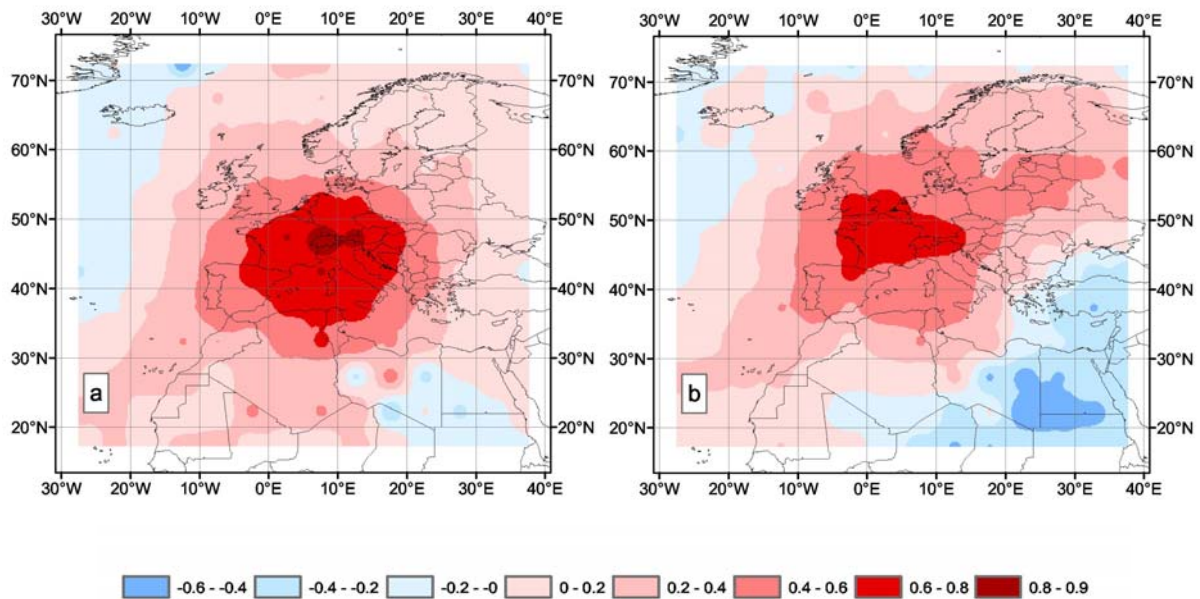


**Fig.3.2.17. Spatial correlation between ALPCLIM 8E-46N gridpoint temperature and European wide CRU time series covering the period 1901 - 1998. a) for summer means (April - September), b) for winter means (October - March)**

The conclusion of the spatial correlation study is clear: instrumental temperature information as well as any proxy information is representative not only for the nearest surroundings of the sites, but also for vast parts of low-elevation Europe.

#### 3.2.4.4. Series of temperature on precipitation days

As already discussed in section 3.1.4 one of the problems in using stable water isotope data from ice cores is caused by the fact, that in the ice-core only temperature information during precipitation events is stored and not temperature of all days (as in the instrumental series). A respective RSC study based on all available daily onsite measurements in the Monte Rosa summit region and on daily meteorological measurements from the regular network in the region in fact showed that there are in fact systematic differences between the instrumental temperatures on all days ( $T_{cli}$ ) minus the temperature during precipitation events ( $T_{prec}$ ). A further refinement of the study showed that the difference is not constant, but depends on the season and also on the precipitation intensity of the event. Regressive models based on the daily RSC-data produced algorithms to calculate the mean monthly differences  $T_{cli} - T_{prec}$  in dependence on the monthly precipitation amounts. These formulas allowed to calculate monthly long-term "precipitation reduced temperature series"  $T_{prec}$  for the ice core sites.

These precipitation reduced sites were considered to be closer linked to stable water isotope series from the ice cores. In fact an analysis of the difference series  $T_{cli} - T_{prec}$  clearly showed (one example for the Monte Rosa grid-point 8E-46N is given by Fig.3.2.18) that there is a systematic and seasonally different bias of  $T_{cli} - T_{prec}$ , it could be demonstrated also, that the long-term trend of that bias is negligible.

In the Monte Rosa case long-term mean  $T_{prec}$  temperatures are 1.25K colder than  $T_{cli}$  in autumn, 0.9K colder in summer, 0.4K colder in autumn and equal to  $T_{cli}$  in winter. But the long-term trend of the bias is zero, only on annual to decadal scale there are minor variations. But those variations are smallest in summer and spring (standard deviation less than 0.1K) and slightly higher (0.25K) in autumn and winter. The conclusion for the most important climate sites of the project on the Colle Gnifetti (Monte Rosa) – where the overwhelming part of the stored snow in the ice cores is spring and summer snow – is, that any temperature trend signals in the ice cores will reflect not only temperature during precipitation events but without any long-term bias (and only extremely small short term noise) also real temperature for all days – therefore comparable to the instrumental temperature series of the region without any precipitation effects. Only the absolute temperature will be shifted by the constant amounts of 0.9K in summer and 0.4K in spring.

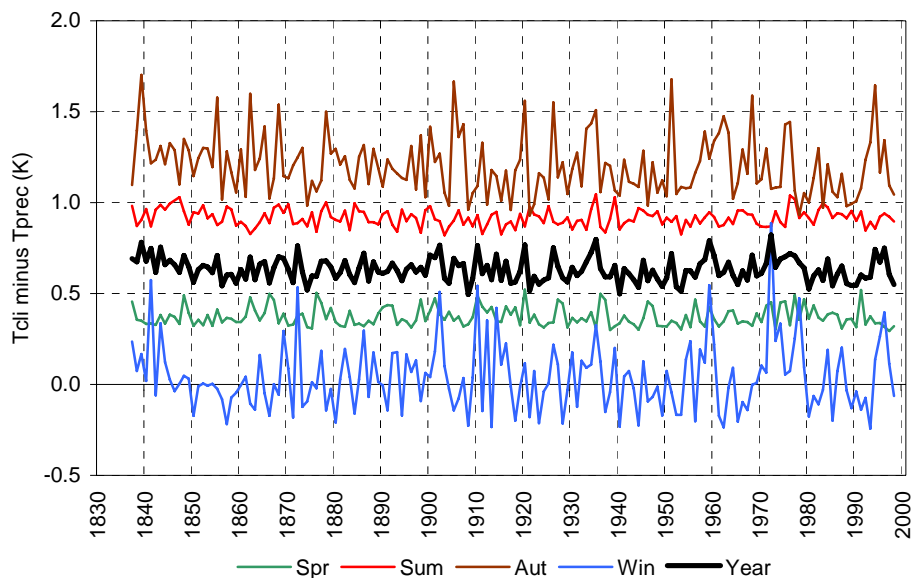


**Fig.3.2.18. Difference series of measured temperature on all days (Tcli) minus precipitation reduced temperature (Tprec) for the high-elevation grid-point 8E-46N (Monte Rosa region) for the four seasons and the year**

### 3.2.4.5. Series of vertical temperature lapse rates

The high elevation ALPCLIM ice core sites in the summit regions of Mont Blanc and Monte Rosa are supposed to provide in background information about a number of atmospheric pollution constituents. The underlying idea why those sites should represent in a certain sense not only local but also large scale pollution features of the air over Europe is mainly based on the assumption that the vertical transport from immediately surrounding low level source regions to the high elevated sites is often hindered by vertically stable stratification of the atmosphere between. The high elevation sites represent the free atmosphere especially in cases when the vertical temperature lapse rates are small and the atmosphere is in a thermally stable condition which hinders vertical uplift of pollutants from the surrounding source regions.

The gridded ALPCLIM high-elevation and low-elevation temperature time series can be used to develop a thermal stability index (TSI) which may be used to better understand the results of chemical analysis of the ice cores. Time series of such a stability index may serve to better separate real trends or variations in the background atmosphere from potential influences of neighbouring source regions. Three TSIs were calculated for each of the ice core sites (MB and MR in Fig.3.2.19) as standardised difference series of the ice core high elevation grid-point temperatures (7E-45N for Mont Blanc, 8E-45N for Monte Rosa) minus three respective low elevation series:

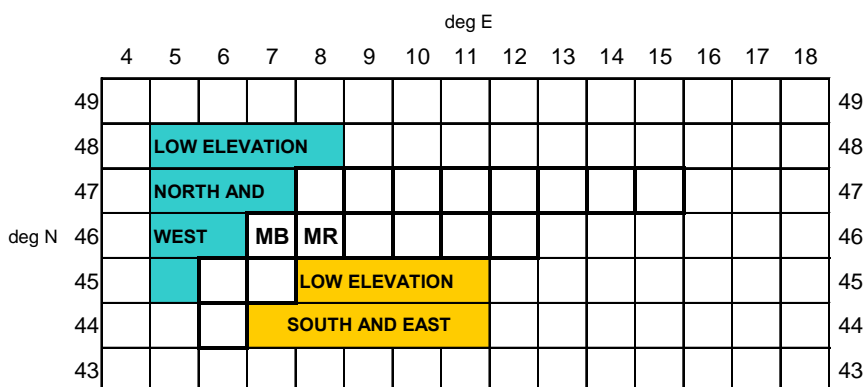


**Fig.3.2.19. Geographical position of the ALPCLIM high elevation ice core sites (MB=Mont Blanc, MR=Monte Rosa) and the two low elevation sub-regions (potential source regions for pollution) used to calculate the thermal stability index TSI**

One for a sub-regional mean “NORTH and WEST” dealing with advection from the northwest (blue in Fig.3.2.19), one for a sub-regional mean SOUTH and EAST dealing with advection from northern Italy (yellow) and one for the respective single low-elevation grid-points of MB and MR. Taking into account the very different vertical lapse rates in the warm and the cold season, the TSI series were calculated for the four seasons and for the summer and winter half years. Figs.3.2.20 and 3.2.21 show the TSI time series for the Mont Blanc and Monte Rosa versus the respective three low elevation sub-regions.

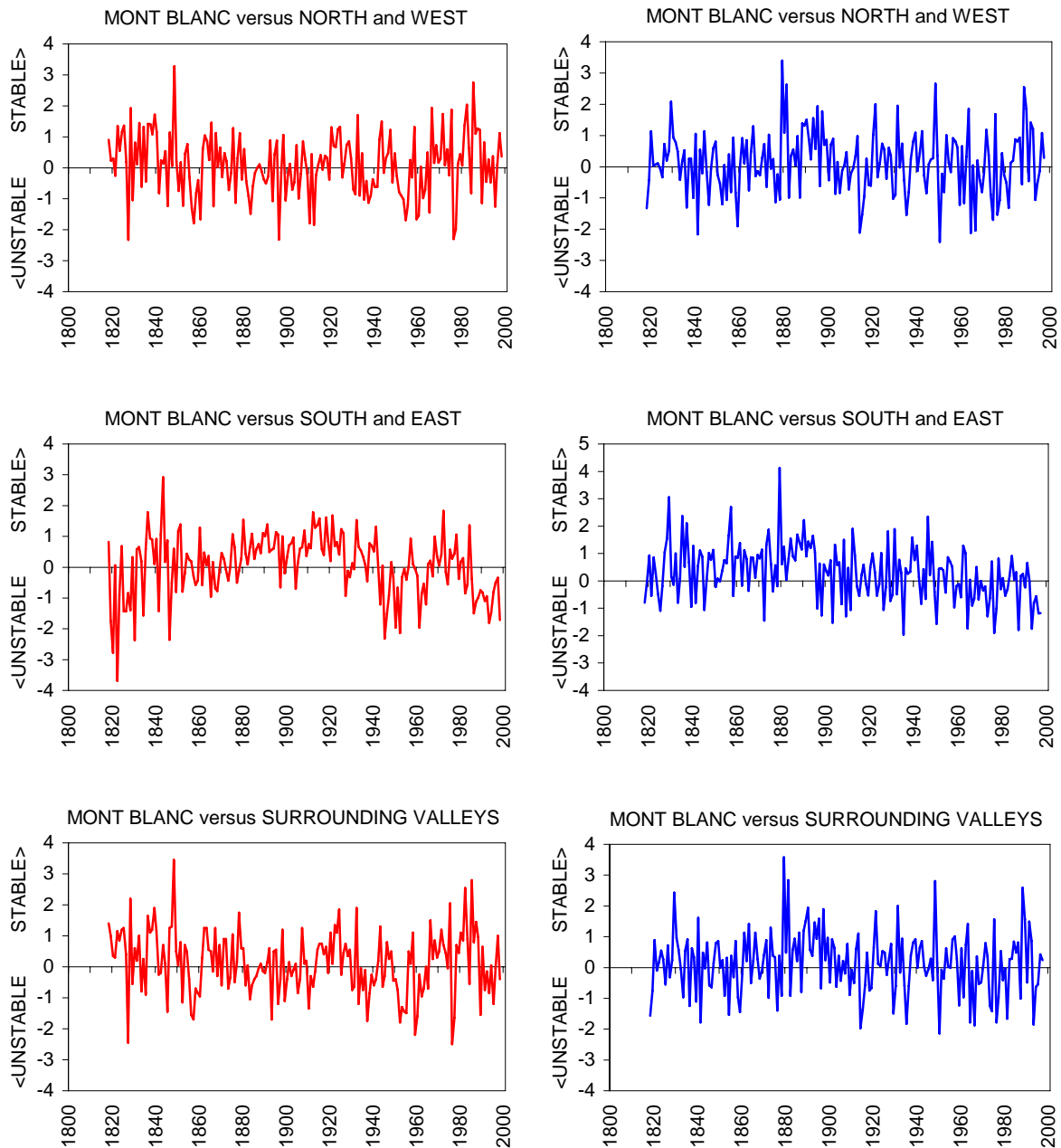


**Fig.3.2.20. Time series of thermal stability index (TSI) MONT BLANC versus LOW ELEVATION SURROUNDINGS left (red): summer half year (months 4 to 9); right (blue): winter half year (months 10 to 3) thermal stability index = standardised vertical temperature lapse rates (high minus low)**

It is evident that (besides the high frequent year to year variability) there have been in fact variations of the TSI at the decadal level as well as even long term trends. TSI series of Mont Blanc and Monte Rosa versus the NW are more characterised by a number of decadal scale variations (e.g. the stable summers of the 1970s and 80s, the stable winters of the 1880s and 1890s or the unstable summers of the 1950s).



The most prominent long-term TSI trends happened (for both MR and MB) versus low elevation northern Italy: In summer there was a long-term shift from unstable to stable from the 1820s to the 1920s, followed by a reverse trend in the 20<sup>th</sup> century – winter stability conditions are characterised by more stable TSI-level in the 19<sup>th</sup> and a long-term trend to more unstable TSIs during the entire 20<sup>th</sup> century.

The TSIs of the high-elevation sites versus the immediately surrounding valleys are a mixture of the NW- and SE-characteristics but they are nearer to the NW- than the SE-features.

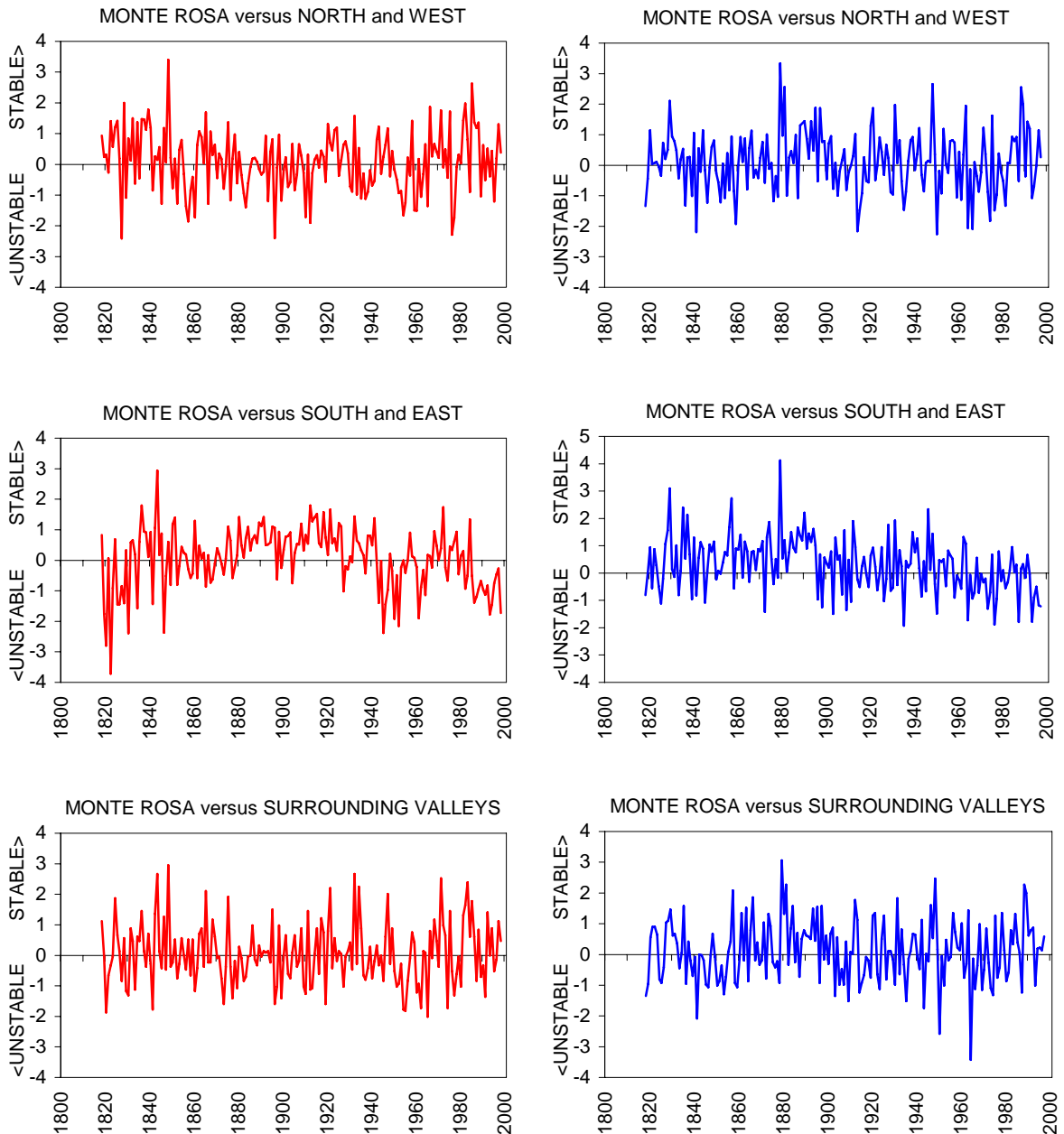


**Fig.3.2.21. Time series of thermal stability index (TSI) MONTE ROSA versus LOW ELEVATION SURROUNDINGS left (red): summer half year (months 4 to 9); right (blue): winter half year (months 10 to 3) thermal stability index = standardised vertical temperature lapse rates (high minus low)**

### 3.2.4.6. Change of the zero degree altitude

Trends and variations of the zero degree altitude in the Alps are interesting for a number of applications in the field of glaciology. A direct deduction of gridded time series of the zero degree altitude from the gridded ALPCLIM temperature dataset is not possible due to too few long-term time series in altitudes above 1500m. If we assume that the mean vertical temperature lapse rates in high altitudes are stable in time relative time series of the changes of the zero degree line can easily be derived by a simple division of the relative temperature changes of a region by the mean vertical lapse rates there. Fig.3.2.22 shows such series for the average of the two high-elevation grid-points of the ice core sites in the Mont Blanc and Monte Rosa region. The mean vertical temperature models were taken from the RSC-study of the project (compare section 3.1.2), the relative temperature series are averaged over the two respective grid-points. The 20<sup>th</sup> century mean zero degree altitude of the region is included in the caption of the vertical axis – allowing a transformation of the relative changes of the series into absolute values. Taking into account the large scale similarity of temperature variability in the entire study region (compare section 3.2.4.1) the relative changes of zero degree altitude in Fig.3.2.22 can be assumed to be representative for larger regions, only the absolute values should only be used for the two site grid-points alone. The described procedure to calculate time series of the zero degree line worked only for those parts of the year with altitudes higher than 1500m. Below 1500m vertical lapse rates are not linear anymore, especially in the cold season, and therefore not appropriate for the described way of proceeding.

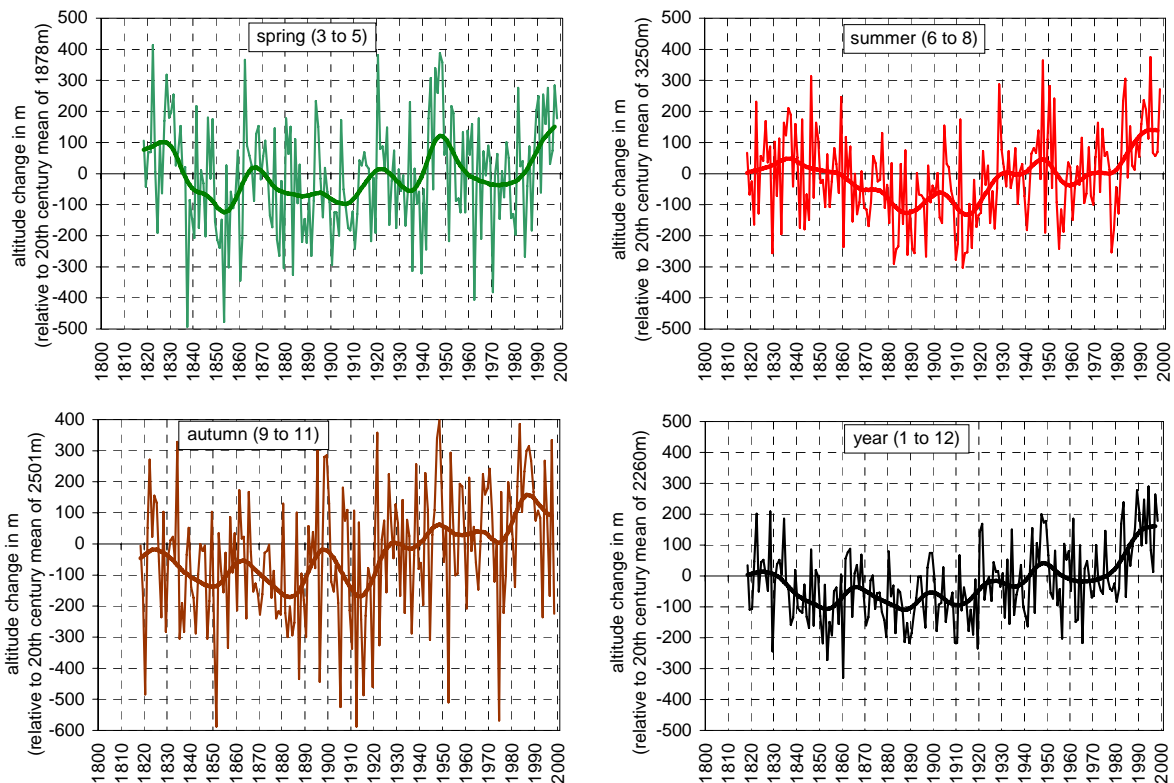


**Fig.3.2.22. Seasonal and annual time series of the zero degree altitude (relative to the 20<sup>th</sup> century mean) for the Monte Rosa and Mont Blanc region (grid-points 7E-46N and 8E-46N)**

Zero degree altitude has increased considerably by approximately 250m since the late 19<sup>th</sup> century. The increase has not been steady due to a number of superposed decadal scale variations. The earlier parts of the series show again higher altitudes – making the early 19<sup>th</sup> century comparable to the recent values especially in the warm season, less for autumn and the annual mean.

### 3.2.5. Conclusions HSC

- A re-analysis of the long-term instrumental temperature and precipitation series of the “Greater Alpine Region” (GAR) in terms of eliminating non-climatic inhomogeneities produced two high quality gridded datasets significantly and systematically different from existing global scale datasets.
- Most of the short-term temperature variability in the GAR is describable by a sub-division into six sub-regions, long-term variability is highly similar in the whole region (also for high- and low-elevation) – but there are considerable seasonal differences.
- Temperature variability in the Alps is representative for large parts of Europe, highly representative for a region ranging from northern Germany to northern Algeria and from western France to mid Hungary in Summer, slightly smaller (and more orientated to the West) in Winter.
- Precipitation variability shows more complicated spatial patterns – there is no single GAR-precipitation series representative for the whole region.
- One of the predominant spatial variability pattern is the “Alpine Seesaw” – a centennial scale oscillation of a dipole structure with two centres of action NW and SE of the Alps
- Time series of “temperature at precipitation days” (which should be closer linked to temperature information from stable water isotopes in ice cores) proved to be similar to “temperature series on all days” at longer time scales but different at short time scales.
- Time series of a “thermal stability index” (TSI) derived from vertical temperature lapse rates between the high elevation ice core sites and different low elevation surroundings showed annual to decadal scale variability only for the low level surroundings in the West and North and the local scale surrounding valleys and no long term trends. TSIs versus the northern Italian source regions on the other hand show also considerable long term trends which may be interesting for the segmentation of the chemistry of the high elevation sites into a “background” and a local signal.
- A simple transformation model from temperature into zero degree line altitude produced time series of the zero degree altitude showing a high annual variability of maximum + - 500m and long term evolutions at the order of +250m from the late 19<sup>th</sup> century to the 1990s.

#### 4. References

- Aschwanden A, Beck M, Häberli Ch, Haller G, Keine M, Roesch A, Sie R, Stutz, M. 1996b. Bereinigte Zeitreihen – Die Ergebnisse des Projekts Klima90, Bd.2: Methoden. *Klimatologie der Schweiz*, Jg.1996, SMA-Zürich, 105 pages
- Auer I, 1993. Niederschlagsschwankungen in Österreich. *Österreichische Beiträge zu Meteorologie und Geophysik*, 7, pp 73, ZAMG, Vienna
- Auer I, Böhm R, Schöner W, Hagen M. 1999. ALOCLIM – Austrian – Central European long-term climate – creation of a multiple homogenized long-term climate data-set. In: HMS-WMO (1999), 47-71
- Auer I, Böhm R, Schöner W. 2001. Austrian long-term climate: Multiple instrumental climate time series in Central Europe (1767-2000). *Österreichische Beiträge zu Meteorologie und Geophysik*, 25, pp 147 plus data-CD, ZAMG, Vienna
- Auer, I. and Schöner, W., 2000: The reliability of precipitation measurements at high mountains – amounts in dependence of instruments and sites, subm. To Proc. Of the third Seminar for Homogenization and Quality Control in Climatological Data Bases, 25 – 29 September 2000, WMO.
- Barry, R.G., 1992: Mountain Weather and Climate, 2<sup>nd</sup> edition. Routledge, London and New York.
- Baumgartner, A., Reichel, E. und Weber, G., 1983: Der Wasserhaushalt der Alpen, München und Wien.
- Böhm, R., I. Auer, M. Brunetti, M. Maugeri, T. Nanni and W. Schöner, 2001: Regional temperature variability in the European Alps 1760-1998 from homogenised instrumental time series. Accepted for: *International Journal of Climatology*
- Böhm R. 1992. Lufttemperaturschwankungen in Österreich seit 1775. *Österreichische Beiträge zu Meteorologie und Geophysik*, 5, pp 96, ZAMG, Vienna
- Böhm R, Auer I, Schöner W, Hagen M. 1998. Long alpine barometric time series in different altitudes as a measure for 19<sup>th</sup>/20<sup>th</sup> century warming. *Preprints of the 8<sup>th</sup> Conference on Mountain Meteorology, in Flagstaff, Arizona*. AMS, Boston, pp.72-76
- Böhm R., Auer I, Briffa K, Brunetti M, Esper J, Grabner M, Haerberli W, Hoelzle M, Hoffmann G, Jones J, Jones PD, Maugeri M, Nanni T, Nicolussi K, Osborn T, Widmann M and R Wimmer, 2001: ALP-IMP: Multi-centennial climate variability in the Alps based on Instrumental data, Model simulations and Proxy data. Proposal EVK2-2001-00241 of a RTD-project to the European Commission, pp 69
- Brown, M.J. and Peck, E.L., 1962: Reliability of precipitation measurements as related to exposure. *J. appl. Met.*, 1, 203-207
- Eischeid, J.K., Diaz, H.F., Bradley, R.S. and Jones, P.D., 1991 “A Comprehensive Precipitation Data Set for Global Land Areas.” Technical Report TR051, 82pp U.S. Dept. of Energy, Carbon Dioxide Research Division.
- Fliri, F., 1974: Niederschlag und Lufttemperatur im Alpenraum. *Wissenschaftliche Alpenvereinshefte* 24, Innsbruck
- Fliri, F., 1984: Synoptische Klimatologie der Alpen zwischen Mont Blanc und Hohen Tauern. *Wissenschaftliche Alpenvereinshefte* 29, Innsbruck
- Frei, C. und Schär, 1998: A Precipitation Climatology of the Alps from High-Resolution Rain-Gauge Observations. *Int. Journal of Climatology* 18:873-900. Chichester.
- Golubev, V.S., 1986: On the Problem of Standard conditions for precipitation gauge installation, in B. Sevruc (ed.) *Proceedings , International Workshop on the Correction of Precipitation Measurements, Instruments and Observing Methods*, Report no.24, (WMO/TD no. 104), 57-59.
- Goodison, B.E., Sevruc, B. and Klemm, S., 1989: WMO solid precipitation measurement inter-comparisons: objectives, methodology, analysis, in W. Delleur (ed) *Atmospheric Deposition*, Int. Assoc. Hydrol. Sci, Publ. No 179, 59-64, Wallingford, UK, IAHS Press.
- Hanssen-Bauer I and Nordli PØ. 1998. Annual and seasonal temperature variations in Norway 1876-1997. *DNMI reports* 25/98, 29 pages
- Havlik, D., 1969 : Die Höhenstufe maximaler Niederschlagssummen in den Westalpen – Nachweis und dynamische Begründung. *Freiburger Geographische Hefte*. Selbstverlag der Geographischen Institute der Albert-Ludwigs-Universität, Freiburg i. Br.
- HMS-WMO. 1997. Proceedings of the 1<sup>st</sup> seminar for homogenisation of surface climatological data. Budapest, 6-12 Oct. 1996, 144 pages
- HMS-WMO. 1999. Proceedings of the 2<sup>nd</sup> seminar for homogenisation of surface climatological data. Budapest, 9-13 Nov. 1998, WCDMP-No.41, WMO-TD No.962, 214 pages
- Hulme, M., 1992: A 1951-80 global land precipitation climatology for the evaluation of General Circulation Models. *Climate Dynamics*, 7, 57-72
- Hulme, M., Osborn, T.J. and T.C. Johns, 1998: Precipitation sensitivity to global warming: Comparison of observations with HadCM2 simulations. *Geophys.Res.Letts.*, 25, 3379-3382
- Jevsons, W.S., 1861: On the deficiency of rain in an elevated rain gauge as caused by wind. *London, Edinburgh and Dublin Phil.Mag.*, 22, 421-433

- Jones, PD. 1994. Hemispheric surface air temperature variations: a reanalysis and an update to 1993. *J.Climate*, **7**, 1794-1802
- Jones PD, New M, Parker DE, Martin S and Rigor IG. 1999. Surface air temperature and its changes over the past 150 years. *Reviews on Geophysics*, **37** 2, 173-199.
- Kirchhofer, K., 1973: Classification of European 500mb patterns. Arbeitsberichte der SMA, 43, Zürich
- Kirchhofer, W., 1971: Abgrenzung von Wetterlagen im zentralen Alpenraum. Arbeitsberichte der SMA, 23, Zürich
- Lütschg, O., 1926: Über Niederschlag und Abfluss im Hochgebirge – Sonderdarstellung des Mattmarkgebietes. Ein Beitrag zur Fluss- und Gletscherkunde der Schweiz. Schweizer Wasserwirtschaftsverband, Verbandsschrift 14. Veröff. Der Hydrologischen Abteilung der SMA in Zürich.
- Maugeri M, Nanni T. 1998. Surface air temperature variations in Italy: recent trends and an updated to 1998. *Theoretical and Applied Climatology* **61**, 191-196.
- Mestre O. 1999. Step by step procedures for choosing a model with change-points. In: HMS-WMO (1999), 15-26
- Moberg, A and Alexandersson H. 1997 Homogenization of Swedish temperature data. Part II: Homogenised gridded air temperature compared with a subset of global air temperature since 1861. *International Journal of Climatology* **17**, 35-54.
- Vose, RS, Peterson TC, Schmoyer RL, Eischeid JK, Steurer PM, Heim RR and Karl TR. 1993. The Global Historical Climatology Network: Long-term monthly temperature, precipitation, and pressure data. *Fourth AMS Symposium on Global Change Studies*, Anaheim, CA., January 17-22 1993
- Peterson TC, Easterling DR, Karl TR, Groisman P, Auer I, Böhm R, Plummer N, Nicholis N, Torok S, Vincent L, Tuomenvirta H, Salinger J, Førland EJ, Hanssen-Bauer I, Alexandersson H, Jones P, Parker D. 1998. Homogeneity Adjustments of In Situ Climate Data: A Review. *International Journal of Climatology* **18**, 1493-1517
- Richman MB. 1986. Rotation of principal components. *J.Climatol.* **6**, 293-335
- Schöner W., Auer I, Böhm R, Keck L and D Wagenbach, 2001: Spatial representativity of air temperature information from instrumental and ice core based isotope records in the European Alps. Accepted for: *Annals of Glaciology*, Vol 35
- Schwarb, M., 1996: Witterungsanalyse anhand der Alpenwetterstatistik mit Bezug auf Niederschlag, Periode 1945-1994. Berichte und Skripten Nr. 58, Geographisches Institut ETH Zürich.
- Schweizerische Meteorologische Anstalt, 1985: Alpenwetterstatistik – Witterungskalender, Beschreibung der einzelnen Parameter, int. Bericht der Abteilung Forschung.
- Szentimrey, T. 1999. Multiple analysis of series for homogenisation (MASH). In: HMS-WMO (1999), 27-46